Biointerface Research in Applied Chemistry
Open-Access Journal (ISSN: 2069-5837)

Article
Volume 15, Issue 5, 2025, 37
https://doi.org/10.33263/BRIAC153.037

Antioxidant Capacity, Inhibitor of Alpha-glucosidase and DPP-IV of Kesambi (*Schleichera oleosa*) Leaf Extract and their Compound Profiles Based on LC-ESI-MS Analysis: *In vitro* and *In silico* Study

Nursamsiar Nursamsiar [1,*], Fitriyanti Jumaetri Sami [1], Henny Kasmawati [2], Syamsu Nur [1], Marwati [3]

[1] Department of Pharmaceutical Analysis and Medicinal Chemistry, Almarisah Madani University, Makassar 90242, Indonesia; nursamsiar@univeral.ac.id (N.); fitriyantijumaetri@univeral.ac.id (F.J.S.); syamsunur@univeral.ac.id (S.N.);
[2] Faculty of Pharmacy, Universitas Halu Oleo, Kendari, Southeast Sulawesi, Kendari 93232, Indonesia; hennykasmawati@uho.ac.id;
[3] Department of Pharmaceutical Biology, Almarisah Madani University, Makassar 90242, Indonesia; marwati@univeral.ac.id;
* Correspondence: nursamsiar@univeral.ac.id;

Received: 14.02.2025; Accepted: 10.05.2025; Published: 8.06.2025

Abstract: Kesambi leaves (*Schleichera oleosa* (Lour.) Oken) are endemic plants spread across Indonesia. Kesambi leaves are empirically used in various traditional medicines. This study aims to evaluate the antioxidant and antidiabetic activities *in vitro* and *in silico*. The dry powder of Kesambi leaves was extracted by sonication using n-hexane, ethyl acetate, acetone, and methanol solvents. The extract was evaluated for its antioxidant capacity using total antioxidant capacity (TAC), cupric ion power reduction (CUPRAC), and ferric reduced antioxidant power (FRAP). The active extract was continued by identifying the compound profile using the LC-ESI-MS approach. The results showed that acetone and ethyl acetate extracts consistently provided strong antioxidant capacity on TAC (478.78 ± 9.48 and 455.44 ± 10.72 mM QEAC/g), CUPRAC (2526.57 ± 23.54 and 1585.15 ± 29.85 mM GAEAC/g), and FRAP (532.99 ± 3.64 and 499.14 ± 7.91 mM QEAC/g). Its alpha-glucosidase and DPP-IV inhibitor activity showed that ethyl acetate and acetone extracts provided significant activity compared to other extracts, with categories ranging from moderate to very strong. Twenty-one compounds were identified in the acetone extract, and eight were identified in the ethyl acetate extract using the LC-ESI-MS approach. Compounds 5, 12, 13, and 14 from acetone extract and compounds 24, 25, and 26 from ethyl acetate extract showed strong interactions with target proteins alpha-glucosidase (2QMJ) and DPP-IV (5T4B) through molecular docking and dynamic approaches. This study provides a scientific description of the ability of Kesambi leaf extract, which has the potential to be an antioxidant and antidiabetic *in vitro* and *in silico*.

Keywords: antioxidant; enzyme inhibition; LC-ESI-MS; reduction capacity; *Schleichera oleosa*.

1. Introduction

Kesambi (*Schleichera oleosa*) is one of Indonesia's native forest plants that have the potential to be used as medicine. Kesambi has active compounds that act as antioxidants. Kesambi (*Schleichera oleosa* (L.) Oken.) is a tropical forest tree plant from the Sapindaceae family, which is spread across South Asia and Southeast Asia (Cambodia, India, Indonesia,

Myanmar, Sri Lanka, Thailand, and Vietnam). In Indonesia, this plant is often found on the island of Java, specifically in the Cilegon and Jember areas. The secondary metabolite content contained in Kesambi (*Schleichera oleosa*) leaves contains flavonoids, alkaloids, tannins, phenols, and steroids. Kesambi (*Schleichera oleosa* (Lour.) Oken) is one of the plants that can be used in medicine, namely as an antioxidant [1].

Various parts of the kesambi plant, such as leaves, fruit, and wood, have been used by people in Java to treat multiple diseases, such as skin diseases, rheumatism, dysentery, acne, stomach aches, and snake stings [2]. The use of Kesambi has been around for a long time. In industry, the oil obtained from the Kesambi fruit can be used as a source of biodiesel [3]. Previous research has stated that Kesambi contains primary metabolite compounds such as sugar, amino acids, protein, and chlorophyll, and its secondary metabolites are alkaloids, terpenoids, phenolic compounds, tannins, flavonoids, etc [4].

Kesambi leaves are known to contain flavonoid and phenolic compounds [5]. Observations on the abaxial part of Kesambi (*Schleichera oleosa*) leaves showed positive results for terpenoids, alkaloids, flavonoids, phenols, tannins, and lipophils [6]. Kesambi leaves extracted using ethanol and ethyl acetate using the reflux method have been reported to contain flavonoids of 62.1 ± 0.98 mgEQ/g (without hydrolysis), 57 ± 0.23 mgEQ/g (hydrolysis), respectively. 40.7±0.77 mgEQ/g (without hydrolysis) and 39.8±0.18 mgEQ/g (hydrolysis) [5].

Another study on Kesambi leaves reported the effect of solvents on the levels of total phenolic and flavonoids in Kesambi leaf extracts. The results of acetone extract were 355.3 ± 3.74 (mgEAG/g), ethyl acetate extract 158.3 ± 3.33 (mgEGA/g), methanol extract 86.2 ± 1.08 (mgEAG/g) and n-hexane extract 18.5 ± 0.45 (mgEGA/g). Meanwhile, the total flavonoid content of Kesambi leaf extract was obtained from ethyl acetate extract 166.3 ± 3.72 (mgEQ/g), acetone extract 61.4 ± 2.60 (mgEQ/g), methanol extract 65.7 ± 0.65 (mgEQ/g), and n-hexane extract 33.7 ± 0.83 (mgEQ/g). The highest total phenolic content was obtained in the acetone extract, and the highest total flavonoid content was obtained in the ethyl acetate extract [7]. The flavonoid compounds in Kesambi leaves are considered very useful in medicine because they are phenolic compounds with strong antioxidant properties. Phenolic compounds are the largest group of compounds that act as natural antioxidants in plants with various pharmacological activities in the form of skin diseases, antioxidants, antidiabetic, antibacterial, and anti-hypertensive [8].

The compound content in plants plays an essential role in their pharmacological activities, such as antioxidants and antidiabetics. Antioxidant activity is the initial stage in developing natural ingredients as medicinal raw materials for treating several degenerative diseases. Several test methods that can be carried out include the 2,2-diphenyl-1-picrylhydrazyl (DPPH), 2,2'-azino-bis-3-ethylbenzothiazoline-6-sulfonic acid (ABTS), and the ferric reducing antioxidant power (FRAP) method. Total antioxidant capacity (TAC), total radical trapping parameter (TRAP), oxygen radical absorbance capacity (ORAC), cupric ion power reducing antioxidant capacity (CUPRAC), Folin-Ciocalteu reducing capacity (FCR test), peroxyl radicals ($ROO^{\bullet}$), superoxide radical anion ($^{-}O_2$), hydrogen peroxide test (H_2O_2), hydroxyl radical test ($^{\bullet}OH$), single oxygen scavenging test ($^{\bullet}O_2$), nitric oxide radical scavenging test ($NO^{\bullet}$) [9]. The method for testing antioxidant activity is based on two inhibitory mechanisms: hydrogen atom transfer (HAT) and single electron transfer (SET). Through this mechanism, a compound that acts as an antioxidant can reduce free radicals into non-reactive and stable molecules, thereby preventing tissue damage caused by excessive exposure to free radicals

[10,11]. The HAT assay is kinetics-based and involves a competitive reaction scheme in which antioxidants and substrates compete for peroxyl radicals generated thermally through the decomposition of azo compounds. ET-based assays measure the capacity of antioxidants to reduce oxidants, which change color when reduced [12]

The antioxidant activity of natural compounds plays a role in various diseases, including diabetes mellitus. Antioxidant compounds play a role in minimizing the effects of increased Reactive Oxygen Species (ROS). ROS modulates the dysfunction of pancreatic beta cells so that insulin production will also be disrupted. Several approaches include dipeptidyl peptidase-IV (DPP-IV) inhibitors as possible agents for treating type 2 diabetes mellitus (T2DM) without causing hyperglycemia and pancreatic β-cell fatigue. DPP-IV inhibitors improve hyperglycemia by stabilizing post-meal gut hormone levels such as glucagon-like peptide-1 and glucose-dependent insulinotropic polypeptide, which function as incretins to help increase insulin secretion and β-cell mass. Another approach is to treat increased postprandial blood sugar levels through an inhibitory approach to alpha-glucosidase. Alpha-glucosidase inhibitors help inhibit or minimize increased blood sugar levels so that the work of the pancreatic beta cells is not forced to release insulin in dealing with increased blood glucose levels. These two approaches can be used as enzymatic testing models to explore natural product candidates as candidates for treating diabetes mellitus [13,14].

This research focuses on testing the potential antioxidant activity of Kesambi leaves using the iron reduction mechanism. These three test methods have advantages, including simple methods, clarity of endpoints and mechanisms, adequate instrumentation, good intra- and inter-test reproducibility, and adaptability for lipophilic and hydrophilic tests simultaneously. They can be widely applied to natural extracts, food, and living creature serum [15]. The antioxidant capacity of the TAC, CUPRAC, and FRAP methods in reducing oxidants can be characterized by a color change when facilitated by a reducing agent as the concentration of the compound in the sample increases. The iron reduction methods are more profitable than other reduction methods due to the reaction of the bis(neocuproin) copper (I) cation chromophore group, which is soluble in water and organic solvents, so that it can test hydrophilic and lipophilic antioxidant activity [16,17]

This study aims to explore Kesambi leaf extract from various solvents as antioxidants and antidiabetics *in vitro*. It is one of the development stages to examine Kesambi leaf extract as an herbal candidate to treat diabetes using an enzymatic approach to DPP-IV and alpha-glucosidase. In addition, information on the antioxidant activity of Kesambi leaf extract using the iron reduction method is still limited, and its relationship to antidiabetic activity with enzymatic methods such as alpha-glucosidase and DPP-4 still needs to be explored further. Hopefully, the results of this study can provide scientific information on the activity of Kesambi extract as an antioxidant and antidiabetic for further research development.

2. Materials and Methods

2.1. Tools and materials.

The tools used include a micropipette (*Dragonlab Micropipette*), Bio red®, an analytical balance (Mettler toledo®), a sonicator, a Shimadzu UV-Vis spectrophotometer (UV-1900), and a rotary evaporator (Buchi®). The materials used included ethanol techniques, ethanol p.a (Merck®), and quercetin (Sigma Aldrich®). H_2SO_4 (Sigma Aldrich®), sodium phosphate (Sigma Aldrich®), ammonium molybdate (Sigma Aldrich®), and $CuCl_2$ (Sigma

Aldrich®). the α-glucosidase from *Saccharomyces cerevisiae* (EC 3.2.1.20) (Sigma Aldrich®), PNPG (Sigma Aldrich®), and DPP-IV enzyme (Sigma Aldrich®)

2.2. Plant collection and extraction.

Kesambi leaves were collected from Takalar Village, Takalar Regency, South Sulawesi, Indonesia (-5.593711618005634,+119.47950235713733). Plant samples were determined at the Plant Anatomy Laboratory, Department of Biology, Makassar State University, with specimen code B-109-UNM. Young kesambi leaves (The leaves are picked in order 3-7 from the shoots) were picked in the morning (07.00-08.00 am, Central Indonesian Time). And cleaned and sorted. The kesambi leaves were then dried in the oven at 40°C three times for 24 hours. Dried samples were sorted and powdered.

The dried powders of Kesambi leaves were weighed as much as 150 grams and extracted using the solvent n-hexane. The residue was re-extracted successively with ethyl acetate, acetone, and methanol by sonication (40 kHz) for 60 minutes at 35°C. The extracts were then filtered, and the filtrate that was obtained was evaporated using a rotary evaporator (Rotavapor® R-300, Buchi Corporation, USA) to obtain a thick extract. The extract obtained was calculated as a percentage (%) of the extract yield.

2.3. Antioxidant capacity testing.

2.3.1. Total antioxidant capacity (TAC) assay.

Kesambi extracts were tested for the total antioxidant capacity of cherry fruit extract and fraction samples according to the procedure [16]. The total antioxidant capacity test is based on the reduction of Mo (VI) ion to Mo (V) ion by the sample, which will form complex bonds in acidic conditions that are green in color. 1 mL of each cherry fruit extract stock solution was pipetted and put into a vial, then mixed in a 4 mL reaction mixture (containing 2 mL of 0.6 M sulfuric acid, 1 mL of 28 mM sodium phosphate, and 1.5 mL of 1% ammonium molybdate) and incubated at 95°C for 10 minutes. After incubation, it was cooled to room temperature, and the absorbance was measured using UV-Vis spectrophotometry at a wavelength of 695 nm. Quercetin solution was used as a standard in preparing the standard curve (1-100µg/mL). The antioxidant activity of samples was determined by the reduction power expressed in QEAC (Quercetin Equivalent Antioxidant Capacity). The potential activity in reducing Mo ions was determined by the formula Equation 1.

$$QEAC = \frac{C \times V \times Fp}{Ws} \quad (1)$$

Equation 1. The formula for determining potential activity in reducing Mo ions was where **C** is the sample concentration, **V** is the final volume, **Fp** is the dilution factor, and **Ws** is the weight of the sample used.

2.1.2. Ferric reducing antioxidant power (FRAP) assay.

The antioxidant activity of Kesambi extract in reducing iron Fe^{3+} to Fe^{2+} was carried out using the FRAP method according to published research procedures [18]. FRAP reagent was prepared by reacting acetate buffer (pH 3.6), TPTZ (0.01 M), and $FeCl_3$ (0.02 M) in a ratio of 10:1:1. A total of 1000 µL of the extract solution was reacted with FRAP reagent and the volume was increased with pro-analysis ethanol to 5 mL in a volumetric flask and incubated at 37°C for 30 minutes. The absorbance of the samples was measured on a UV-visible

spectrophotometer (596 nm). Quercetin was used as a standard to obtain a standard curve equation, which was calculated at a series of concentration ranges of 1-10 µg/mL. Determination of antioxidant capacity was equivalent to quercetin in 1 gram of extract (QEAC/g extract). The potential activity in reducing Fe ions was determined by the formula Equation 1.

2.4. Alpha-glucosidase enzyme inhibition activity assay.

Into the well plate 96, 130 µL of phosphate buffer solution pH 6.8 (Blank Control) was added, 100 µL of phosphate buffer solution pH 6.8 was added, 30 µL of α-glucosidase enzyme 0.075 U/mL (Control), 100 µL of sample, and 30 µL of phosphate buffer 6.8 (Blank Sample), 100 µL of sample, and 30 µL of α-glucosidase enzyme 0.075 U/mL (Sample). Each mixture was then incubated at 37°C for 10 minutes. Each mixture was added 30 µL of PNPG substrate (5 µM), then incubated again for 10 minutes at 37°C. After the incubation process, 90 µL of 0.2 M Na_2CO_3 solution is added, and the absorbance is measured using the microplate reader at a wavelength of 405 nm [19]. Blank and sample controls (without added enzyme and substrate) were measured to avoid false-positive results. Calculation of IC_{50} using regression equation (y = ax + b) the following formula:

$$\% \text{ Inhibition} = \frac{(\textbf{abs blank} - \textbf{abs blank control}) - (\textbf{abs sample} - \textbf{abs sample control})}{\textbf{abs blank} - \textbf{abs blank control}} \times 100 \quad (2)$$

2.5. Dipeptidyl peptidase enzyme inhibition activity assay.

The test of the activity for DPP-IV Inhibition was performed by using a microplate 96-well method, as described previously by [20]. Preparation consists of the sample, sample control, blank, and blank control. To prepare the sample, a weighed quantity of the test sample was dissolved in Tris HCl buffer pH 7.5 to prepare a solution to create five concentration series within the valid range. Test samples (35 µL each) were taken and mixed with 15 µL DPP-IV enzyme and incubated at 37°C for 10 minutes. After incubation was over, 50 uL of Gly-pro-p-nitroanilide (GPPN) substrate 1,2 mM was added and incubated for 30 minutes. To stop the reaction, 25 µl of asam asetat glacial 30% was added. To prepare the sample control, use the same procedure as the sample preparation but without adding the DPP-IV enzyme. To prepare the blank, use the same procedure as the sample preparation but without the sample solution. To prepare the blank control, use the same procedure as the blank solution without adding the DPP-IV enzyme. The solution was then assayed for absorbance at 405 nm. Calculation of IC_{50} using regression equation (y = ax + b) the following formula:

$$\% \text{ Inhibition} = \frac{(\text{abs blank} - \text{abs blank control}) - (\text{abs sample} - \text{abs sample control})}{\text{abs blank} - \text{abs blank control}} \times 100 \quad (3)$$

2.6. LC-ESI-MS analysis.

Each 5µL extract was injected into the LC-ESI-QTOF system. The LC was connected to a QTOF mass spectrometer coupled to the ESI. The ESI parameters were capillary temperature 120°C, atomizer gas 50 L/hour, and source voltage +2.9 kV. Solvent A was five mM ammonium formate; solvent B was 0.1% formic acid in acetonitrile. The solvent was set at a 0.4 mL/min flow rate. All conditions for using LC-ESI-MS were adjusted according to the procedures of [11]. The identification of compounds by LC-MS/MS from each extract was

visualized as a chromatogram. Identified compounds were analyzed using Masslinx software and confirmed using web tools: https://www.chemspider.com/StructureSearch.

2.7. Molecular docking evaluation.

Molecular docking studies were performed using alpha-glucosidase (PDB ID 2QMJ) and DPP-IV (PDB ID 5T4B) proteins obtained from the Protein Data Bank (https://www.rcsb.org/). In the docking simulation carried out using AutoDockTools v.1.5.7 software, the grid was formed with box dimensions (26x22x38) Å with grid box coordinates (x, y, z) 37.692 Å, 50.549 Å, and 40.712 Å on the DPP-4 enzyme. And a grid box (40x40x40) Å with grid box coordinates (x, y, z) -21.727 Å, -6.323 Å, -5.28 Å for alpha-glucosidase. The grid was formed at the location of the bound ligand structure, after which information about the target-ligand protein and grid dimensions was saved in a file format (*.gpf). In electrostatic potential, the AutoGrid 4.2 grid map and the calculation results will be saved in the format (*.glg). Then, the docking tools were selected, and Lamarckian GA was selected and saved in file format (*.dpf). The docking simulation results are saved in a file format (*.dlg) [21].

2.8. Molecular dynamics evaluation.

The stability of the interaction between the ligand and the target protein was evaluated by molecular dynamics (MD) using YASARA software (YASARA Bioscience GmBH, Vienna, Austria), as has been done by Aristianti *et al*. [22]. The parameters evaluated include root mean square deviation (RMSD), root mean square fluctuation (RMSF), and radius of gyration (RoS).

2.9. Statistical analysis.

The antioxidant activity of each sample was expressed as the mean + SD, which was repeated three times. LC-ESI-MS analysis data were characterized using Masslynx Software V4.1 version.

3. Results and Discussion

3.1. Extraction yield.

Extraction of kesambi leaves, which is carried out modernly and involves cavitation waves using sonication techniques, has succeeded in extracting the chemical components contained in kesambi leaves. The ultrasonic-assisted extraction method was used because several reports show that it occurs quickly, the solvent is not large, and it can produce large yields [23]. Overall, it shows that the extract obtained was <10%, meaning the yield was quite low. This case differs from several theories showing that the sonication extraction method can produce relatively large yields. The results of this research still need to be studied regarding the extraction method used. However, this study carried out a multilevel extraction process with various solvents based on their polarity level. The extraction process begins using non-polar to polar solvents, namely n-hexane, followed by ethyl acetate, acetone, and methanol. This multi-stage extraction process was carried out to extract compoundsccording to their respective polarities, and the target compound could be evaluated [24,25]. Based on the yield results (%) obtained, acetone extract tends to have a more excellent yield value than extracts using other solvents **(**Table 1**)**. It is assumed that the compounds from Kesambi leaf extract

tend to be semipolar. From this study, it can be assumed that the effectiveness of the extraction process is determined by the method used and the extraction solvent chosen. Each of the extracts obtained was evaluated for its bioactivity as an antioxidant to observe the ability of an extract to reduce transition metals.

Table 1. The yield (%) of Kesambi leaf extract.

No	Solvent	Sample weight (g)	Extract (g)	Yield (%)
1	n-hexane	150	1.72	1.15
2	Ethyl Acetate		2.44	1.62
3	Acetone		4.79	3.19
4	Methanol		2.26	1.51

3.2. Antioxidant activity.

The antioxidant activity of Kesambi leaf extracts was evaluated using various testing methods, namely total antioxidant capacity (TAC), FRAP, and CUPRAC assay. All three of these methods were carried out colorimetrically using UV-visible spectrophotometry, and the color changes caused by the reduction of transition metals (Fe (III), Cu (II), and Mo (VI)) were evaluated. The results of evaluating the antioxidant activity profile of ethyl acetate and acetone extracts from Kesambi leaves are presented in Table 2.

Table 2. The antioxidant capacity results of each extract in reducing transition metals.

Kesambi leaf extract	TAC Assay (mM QEAC/g extract)	CUPRAC Assay (mM GAEAC/g extract)	FRAP Assay (mM QEAC/g extract
n-hexane extract	279.67±2.20*^{d}	1542.58±8.44*^{b}	382.73±5.89*^{d}
Ethyl Acetate extract	455.44±10.72*^{c}	1585.15±29.85*^{a}	499.14±7.91*
Acetone extract	478.78±9.48*^{b}	2526.57±23.54*	532.99±3.64*
Methanol extract	258.28±8.43*^{a}	1277.07±74.25*	346.80±10.38*^{a}

*indicates that the antioxidant activity of the extracts is significantly different ($p<0.05$, LSD, n=3); ^{abcd} indicates that the alphabetical differences indicate no significant difference between the extracts ($P>0.05$, LSD, n=3).

The resulting antioxidant potential in Table 2 shows a correlation in the reducing ability of each method. The antioxidant activity of each extract in reducing Mo(VI) to Mo(V) indicates that Kesambi leaf acetone extract provides the highest reduction power of 478.78 ± 9.48, followed by ethyl acetate, n-hexane, and methanol extracts, each at 455.44. ±10.72, 279.67±2.20, and 258.28±8.43 mM QEAC/gram extract. The higher the QEAC value of the extract, the more significant the reduction power. Similar results were also obtained in testing antioxidant activity in reducing Fe^{3+} to Fe^{2+} via the FRAP assay and Cu^{2+} to Cu^{+} via the CUPRAC assay. The highest reduction ability was shown in acetone, ethyl acetate, n-hexane, and methanol extracts of Kesambi leaves (Table 2). The FRAP and CUPRAC methods showed reduction powers similar to those of the TAC method. The reduction ability of each method and the fact that it provides the same strength profile are most likely due to the compound molecules in each extract having similar reduction abilities. The activity of acetone and ethyl acetate extracts is strongly suspected to have strong redox capabilities, so these extracts can be used as active antioxidant ingredients.

Evaluation of antioxidant activity using the TAC, FRAP, and CUPRAC methods is the type of test most often used to describe the redox ability of test compounds [26]. The TAC method is widely used for biological samples to estimate extracellular non-enzymatic antioxidants. Apart from that, in principle, the TAC method is a direct method for testing antioxidant activity because it directly inhibits the oxidation of a compound. The application of the TAC method involves thermals, which aim to produce a stable radical flux in solution. Therefore, this method is excellent for measuring extracts' antioxidant activity[27,28]. This

differs from the FRAP and CUPRAC methods, which are antioxidant measurement methods using indirect principles. However, the formation of the reduction reaction has the same principles, even in different media. Antioxidant activity with the FRAP method involves the Fenton reaction mechanism, while the CUPRAC assay involves the Haber-Weiss reaction mechanism. Iron and copper in biological systems can trigger the formation of Reactive Oxygen Species (ROS), which will cause various disorders and certain diseases [28,29].

The three methods (TAC, CUPRAC, and FRAP) to measure antioxidant capacity have provided a correlated profile. The antioxidant activity of Kesambi leaf extract also has the same ability to reduce DPPH radicals. Previous studies also showed that extracts from kesambi leaves have very strong antioxidant activity (<50 µg/mL) in inhibiting DPPH activity [30,31]. In principle, it involves reduction and oxidation mechanisms and electron transfer (ET) mechanisms between compounds that act as antioxidants and towards substrates or oxidants [32,33]. Several compounds, including phenolics and flavonoids, which are mainly obtained from plant extracts, have been proven to have suitable redox mechanisms so that these compounds can act as natural antioxidants [34]. To correlate this theory, this study characterized secondary metabolite compounds from acetone and ethyl acetate extracts to describe the most likely compounds that act as antioxidants in reducing iron.

3.3. Antidiabetic activity.

Antidiabetic activity testing was carried out with the parameters of inhibition of α-glucosidase enzyme and DPP4 enzyme. Alpha-glucosidase and DPP-IV enzymes are both important parameters for evaluating the ability of a compound to provide anti-diabetic effects *in vitro*. Alpha-glucosidase plays a role in converting carbohydrates into glucose [35,36]. In contrast, DPP-IV plays a role in increasing the degradation of GLP-1, which is the endogenous incretin hormone glucagon-like peptide-1 associated with the disposal of glucose from the intestine [37]. Both enzymes are interconnected in improving blood sugar levels and are associated with diabetes mellitus. Therefore, extracts from Kesambi leaves are expected to have the ability to inhibit or slow down the activation of these enzymes naturally.

Kesambi leaf extracts, including n-hexane, ethyl acetate, acetone, and methanol extracts, were studied for their ability as antidiabetics, especially in inhibiting alpha-glucosidase and DPP4 (Table 3). The results showed that Kesambi leaf extract could inhibit α-glucosidase enzyme with activity values (IC_{50}) for n-hexane, ethyl acetate, acetone, and methanol extracts of 99.3236±0.16; 72.87±0.78; 1.6798±0.28; and 24.46533±0.37 µg/mL, respectively, while for DPP4 enzyme were 232.5±1.86; 83.14±0.75; 307.92±2.46. However, no inhibitory effect was found on the DPP-4 enzyme in the n-hexane extract. The best activity was shown in the acetone extract for α-glucosidase and DPP4 enzymes.

Table 3. Antidiabetic activity (IC_{50}).

Kesambi leaf extract	α-glukosidase (µg/mL)	DPP4 (µg/mL)
n-hexane extract	99.32±0.16*	nd
Ethyl Acetate extract	72.87±0.78*	232.52±1.86*
Acetone extract	1.6798±0.28*	83.14±0.75*
Methanol extract	24.46533±0.37*	307.92±2.46*

nd: nondetermination; *showed significantly different each extract (p-value <0.05, LSD)

In vitro, it was shown that the acetone extract can inhibit both alpha-glucosidase and DPP-IV enzymes. The ability of acetone extract is assumed that there are compounds with medium to high polarity that can inhibit the enzyme's activity. Compounds from the phenolic

and flavonoid groups play a significant role in its activity in inhibiting alpha-glucosidase and DPP-IV [37]. Kesambi leaf extract has been reported to be rich in phenolic or flavonoid compounds. Several studies have reported that phenolic or flavonoid compounds actively inhibit alpha-glucosidase and DPP-IV enzymes [38]. The possible mechanism that occurs is the interaction of hydrogen in phenolic compounds with enzymes that can inactivate the catalytic ability of the active side of the enzyme. In addition, metalloenzymes from alpha-glucosidase and DPP-IV can be targeted for the complexation of phenolic or flavonoid compounds, so it will reduce the performance of both enzymes, thereby reducing blood sugar levels [38,39]. The activity of alpha-glucosidase and DPP-4 inhibitors in the Kesambi extract may be linked to its antioxidant properties. Figure 1 illustrates the relationship between antioxidant activity and the inhibitory effects on alpha-glucosidase and DPP-4.

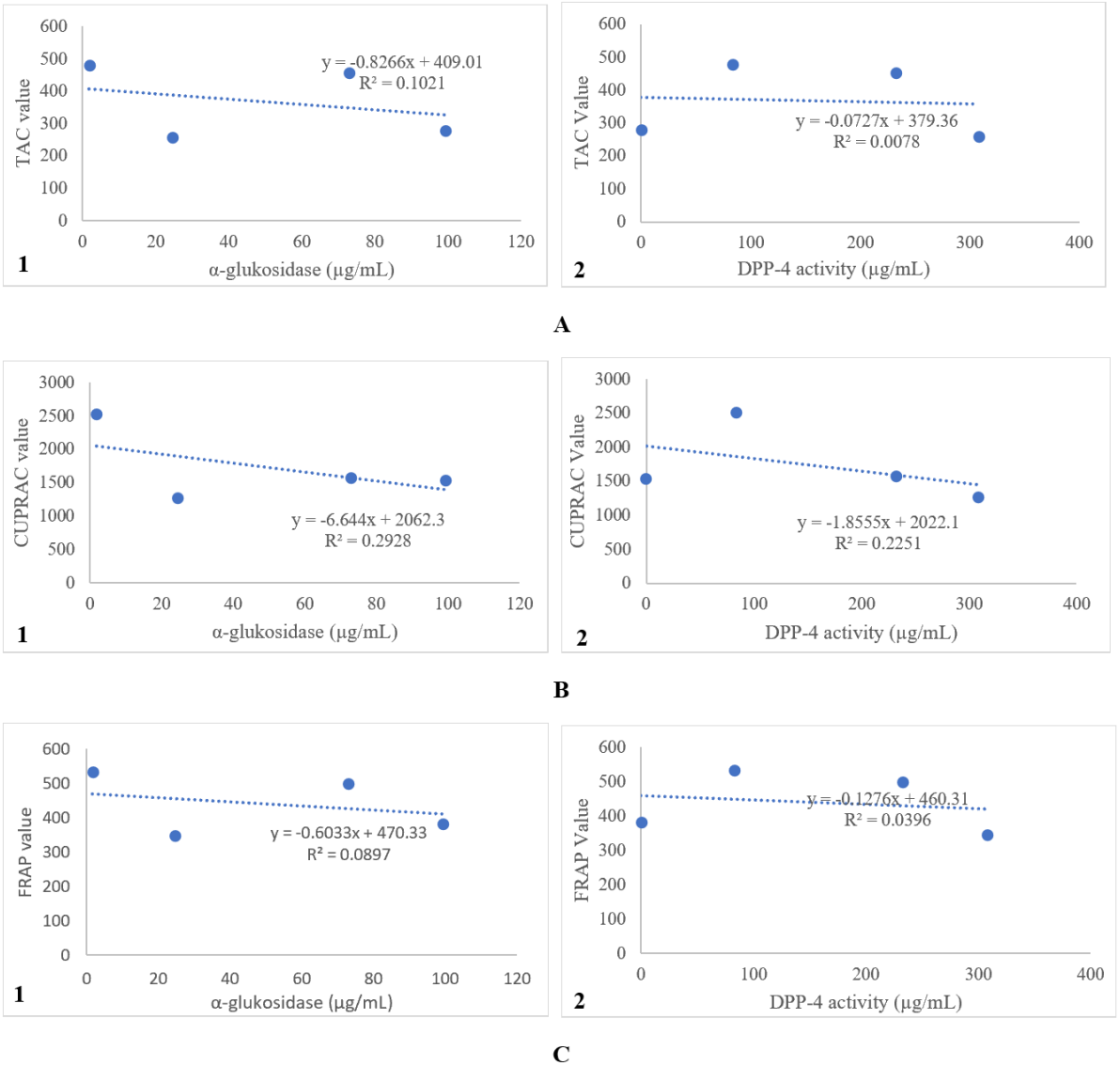

Figure 1. Correlation between antioxidant activity using the **(A)** TAC; **(B)** CUPRAC; **(C)** FRAP methods on the activity of kesambi leaf extract in inhibiting **(1)** α-glucosidase; **(2)** DPP-4.

The ability of Kesambi leaf extract to inhibit α-glucosidase and DPP-4 shows a weak correlation with the extract's antioxidant activity (Figure 1). The antioxidant activity of each extract is not entirely responsible for the inhibition mechanism of α-glucosidase and DPP-4. The percentage of the relationship between the two ranges from 10-30%, which means that only up to 30% of the extract's ability as an antioxidant affects the inhibition of the α-glucosidase and DPP-4 enzymes. The occurrence of a weak correlation between the antioxidant

activity of the extract against a-glucosidase and DPP-4 still needs to be evaluated further. With the principle of iron reduction evaluated in this study, the antioxidant activity may not be by the target mechanism. It is necessary to evaluate the antioxidant activity with other mechanisms, such as the radical scavenging mechanism, which is directly associated with the ROS mechanism, as ROS modulates the occurrence of pancreatic beta cell dysfunction related to overexpression of DPP-4 [13,14].

3.4. Phytochemical composition.

Compound characterization was carried out using LC-ESI-MS. The identified compounds in acetone and ethyl acetate extracts from Kesambi leaves can be seen in Figure 2. The results of acetone extract analysis using LC-ESI-MS produced **21** compounds (chromatogram peaks) in the retention time range of 4-20 minutes (Figure 2A). Interpretation of compounds from chromatogram peaks using MassLynx software (Version 4.1) and identification of the structure of chemical compounds detected on LC-ESI-MS with the online Mass Bank database. Of the 13 peaks analyzed, compounds from the alkaloids, phenolics, flavonoids, coumarins, lactones, and lignin derivatives were identified (Table 4). From this group of compounds, likely, the compounds containing **(**1R,3R,4S,5R)-3-[(E)-3-(3,4-dihydroxy phenyl) prop-2-enoyl] oxy-1,5-dihydroxy-4-[(E)-3-(3-hydroxy-4-methoxy phenyl) prop-2- noyl] oxycyclohexane-1 carboxylic acid, which was phenolic compounds, rhoifolin, cianidanol and 5,7-Diacetoxy-3,4',8-trimethoxyflavone were flavonoid compounds, and dicoumarol which was a coumarin compound provide a role as an antioxidant. Based on its chemical structure, this compound contains a hydroxyl group in the aromatic core, thus allowing radical scavenging or reduction of transition metals through electron transfer and hydrogen atom transfer mechanisms [32,40]. Compounds from other groups identified in Kesambi leaf acetone extract do not have electrons or hydrogen that can be donated to radicals or redox mechanisms. However, this condition still needs to be studied more deeply for these compounds.

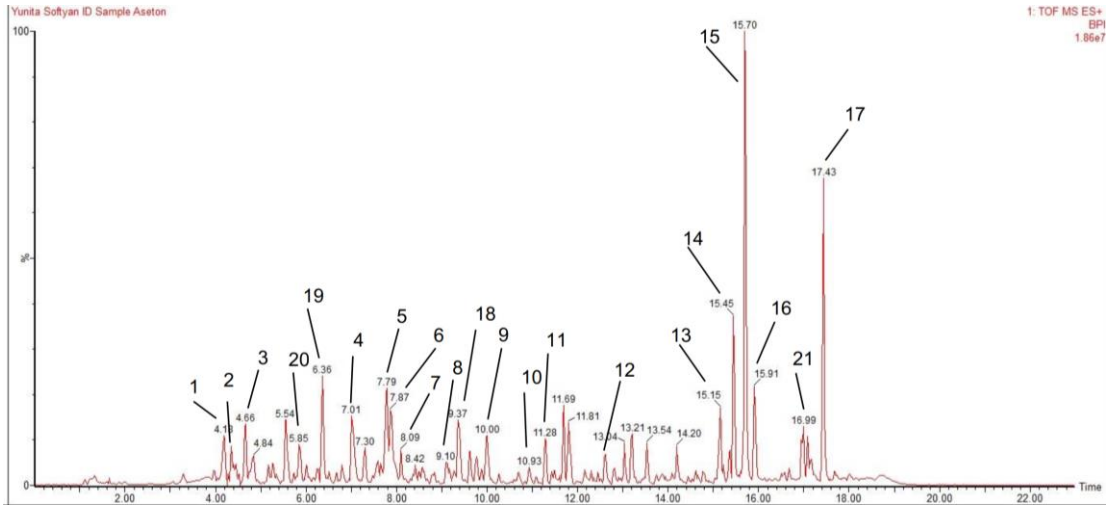

(a)

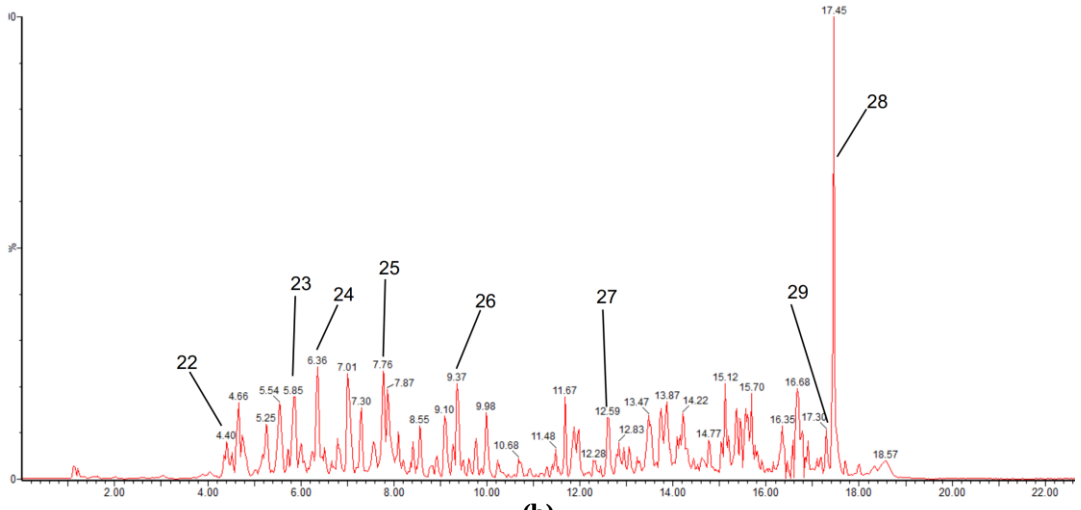

(b)

Figure 2. UPLC spectrum of **(a)** Kesambi acetone extract; **(b)** Kesambi leaf ethyl acetate extract. Compounds with the symbol (*) in Figure 2 have corresponding chemical names in Table 4.

Table 4. Phytochemical composition of Kesambi leaf extract based on LC-ESI-MS results.

No	RT (min)	Observed MS (m/z) [M+H]	Compounds	Molecular formula	Extract	Group
1	4.18	387.16	Colchiceina	$C_{21}H_{23}NO_6$	**Acetone extract**	Alkaloid
2	4.28	290.2681	D-(+)-Catechin	$C_{15}H_{14}O_6$		Flavonoid
3	4.66	580.17	Rhoifolin	$C_{27}H_{30}O_{14}$		Flavonoid
4	7.01	578.19	Podophyllotoxin glucoside	$C_{28}H_{32}O_{13}$		Lignan derivate
5	7.79	576.18	(1R,3R,4S,5R)-3-[(E)-3-(3,4-dihydroxy phenyl) prop-2-enoyl] oxy-1,5-dihydroxy-4-[(E)-3-(3-hydroxy-4-methoxy phenyl) prop-2- noyl] oxycyclohexane-1 carboxylic acid	$C_{28}H_{30}O_{13}$		Phenolic
6	7.87	429.39	5,7-Diacetoxy-3,4',8-trimethoxyflavone	$C_{22}H_{20}O_9$		Flavonoid
7	8.09	576.5459	Podophyllotoxin β-D-glucoside	$C_{28}H_{32}O_{13}$		Lignan Glicoside
8	9.10	182.12	Undeca-2,4,6-trienoic acid	$C_{11}H_{16}O_2$		Lipid acid
9	10.00	415.40	(-)-Podophyllotoxin	$C_{22}H_{22}O_8$		Lignan derivate
10	10.93	337.3	Dicoumarol	$C_{19}H_{12}O_6$		Coumarin
11	11.28	315.4913	MFCD00152656	$C_{18}H_{37}NO_3$		Amida
12	12.62	519.640	N-[(2S)-4-Amino-1-{[(2S)-1-amino-5-carbamimidamido-1-oxo-2-pentanyl]amino}-1-oxo-2-butanyl]-N^2-(phenylacetyl)-L-lysinamide	$C_{24}H_{41}N_9O_4$		Peptida
13	15.15	618.884	(3β,16α,21β,22α)-16,21,22,24,28-Pentamethoxyolean-12-en-3-yl acetate	$C_{37}H_{62}O_7$		Triterpenoid
14	15.45	608.6835	2-[4-(Diphenylmethyl)-1-piperazinyl]ethyl methyl 2,6-dimethyl-4-(3-nitrophenyl)-3,5-pyridinedicarboxylate	$C_{35}H_{36}N_4O$		Piridin
15	15.70	593.28	Pheophorbid	$C_{35}H_{36}N_4O_5$		Chlorophyll derivate
16	15.91	592.676	Bis[2-(4-butoxyphenoxy)ethyl] (4-hydroxybenzylidene)malonate	$C_{34}H_{40}O_9$		Malonate
17	17.43	620.737	L-Phenylalanine, N-[[(3S)-2-[(2S)-2-amino-3-(4-hydroxyphenyl)-1-oxopropyl]-1,2,3,4-tetrahydro-3-isoquinolinyl]methyl]-L-phenylalanyl	$C_{37}H_{40}N_4O_5$	**Acetone Extract**	Peptida
18	9.37	416.14	Dulxanthone G	$C_{22}H_{22}O_8$		Phenolic
19	6.36	592,55	6-[(1,3-Dihydroxy-2- propanyl)ami no]-12-(D-glucopyranos yl)-2-hydroxy- 12,13-dihydro-5H-indolo[2,3-]pyrrolo[3,4 -c]carbazole- 5,7(6H)-dione	$C_{29}H_{28}N_4O_{10}$		Alkaloid glicoside
20	5.85	197,23	L-Histidine trimethylbetaine	$C_9H_{15}N_3O_2$		Kuarterner amonium
21	16,99	620.7292	Nimbolinin D	$C_{36}H_{44}O_9$		Nimbolinins
22	4.40	450.11	Quercitrin	$C_{21}H_{20}O_{11}$	**Ethyl acetate**	Flavonoid
23	5.85	198.12	Loliolide	$C_{11}H_{16}O_3$		Lactone
24	6.36	593,1915	Linarin	$C_{28}H_{32}O_{14}$		
25	7.76	576.19	(1R,3R,4S,5R)-3-[(E)-3-(3,4-dihydroxy phenyl) prop-2-enoyl] oxy-1,5-dihydroxy-4-[(E)-3-(3-	$C_{28}H_{30}O_{13}$		Phenolic

No	RT (min)	Observed MS (m/z) [M+H]	Compounds	Molecular formula	Extract	Group
			hydroxy-4-methoxy phenyl) prop-2- noyl] oxycyclohexane-1 carboxylic acid			
26	9.37	416.14	Dulxanthone G	$C_{22}H_{22}O_8$		Phenolic
27	12.59	630.46	Annohexocin	$C_{35}H_{64}O_9$		Tetrahydrofuran lactone
28	17.45	628.8773	Muricoreacin	$C_{35}H_{64}O_9$		Tetrahydrofuran lactone
29	17.3	580.46	Corossolone	$C_{35}H_{62}O_6$		Tetrahydrofuran lactone

Note: 21 compounds have been identified in the acetone extract, while 8 compounds were successfully obtained from the ethyl acetate extract of Kesambi leaves.

Ethyl acetate extract from Kesambi leaves also provides a strong antioxidant activity profile. The content of secondary metabolite compounds from the ethyl acetate extract was also characterized using LC-ESI-MS. The results showed that eight **(8)** compounds had been identified. In the ethyl acetate extract of Kesambi leaves, it was determined that there were compounds in the phenolic group, flavonoids, and lactones. The phenolic compound contained Dulxanthon G and **(**1R,3R,4S,5R)-3-[(E)-3-(3,4-dihydroxy phenyl) prop-2-enoyl] oxy-1,5-dihydroxy-4-[(E)-3-(3-hydroxy-4-methoxy phenyl) prop-2- noyl] oxycyclohexane-1 carboxylic acid, while the flavonoid group contained quercitrin (Figure 2B). Other compounds are lactone derivatives, namely loliolide, Annohexocin, and corossolone. Compound (1R,3R,4S,5R)-3-[(E)-3-(3,4-dihydroxy phenyl) prop-2-enoyl] oxy-1,5-dihydroxy-4-[(E)-3 -(3-hydroxy-4-methoxyphenyl) prop-2- enoyl]oxocyclohexane-1 carboxylic acid, which was a phenolic derivative, was predicted to be found in acetone and ethyl acetate extracts from kesambi leaves. The presence of quercitrin, dulxanthon G and **(**1R,3R,4S,5R)-3-[(E)-3-(3,4-dihydroxy phenyl) prop-2-enoyl] oxy-1,5-dihydroxy-4-[(E)-3-(3-hydroxy-4-methoxy phenyl) prop-2- noyl] oxycyclohexane-1 carboxylic acid compounds in ethyl acetate extract, which have a hydroxyl (OH) group in the aromatic, also plays a role in the electron or proton donor mechanism so that reduction reactions of transition metals such as Fe, Cu, and Mo can occur [39]. The chemical structure of the suspected antioxidant compounds from acetone and ethyl acetate extracts of Kesambi leaves can be seen in Figure 3.

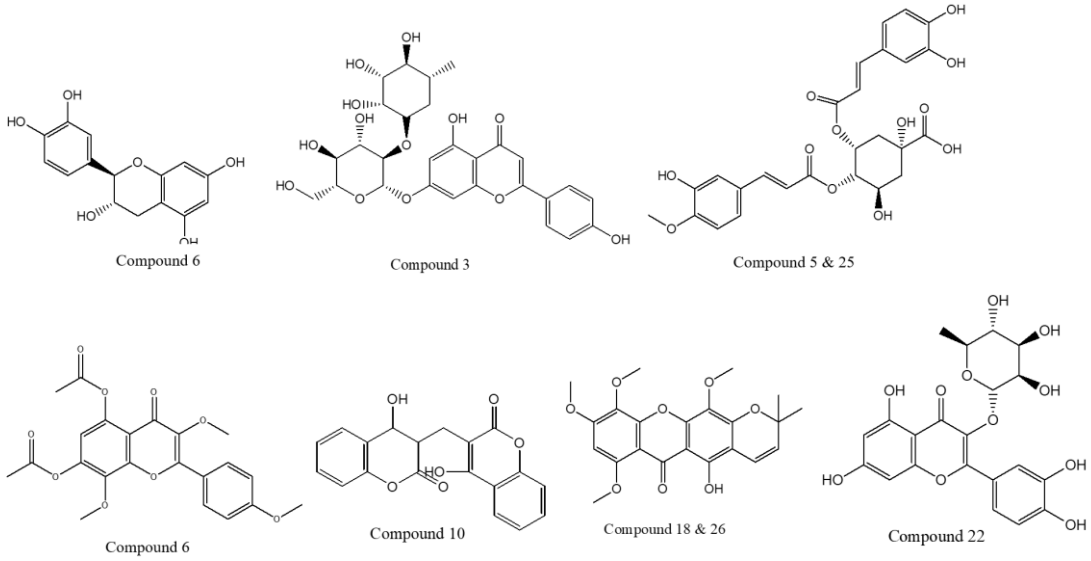

Figure 3. Chemical structure of active compound prediction of *A. flava* extract as an antioxidant. The numbering of the compounds in the figure is adjusted to the order of the compounds in Table 4.

Phenolics and flavonoids are exogenous antioxidants that have been proven helpful in preventing cell damage due to oxidative stress. The mechanism of action of phenolics and flavonoids as antioxidants can be direct or indirect [41]. Phenolic/flavonoids act as antioxidants directly by donating hydrogen ions to neutralize the toxic effects of free radicals [33,41]. Meanwhile, phenolic/flavonoids act as antioxidants indirectly by increasing endogenous antioxidant genes' expression through several mechanisms. One mechanism for increasing antioxidant gene expression is through activation of nuclear factor erythroid two relating factor 2 (Nrf2), increasing genes that play a role in the synthesis of endogenous antioxidant enzymes, such as the SOD (superoxide dismutase) gene [42]. Meanwhile, according to Nur *et al*., phenolic compounds have a mechanism as antioxidants, namely through the ability of the phenol group to bind a free radical by donating its hydrogen atom through an electron transfer process so that the phenol turns into a phenoxyl radical [10].

3.5. Molecular docking evaluation.

An *in silico* test was conducted on 29 compounds successfully identified from ethyl acetate and acetone extracts of Kesambi leaves. The 29 compounds were evaluated for their chemical molecular interactions with DPP4 and α-glucosidase enzymes. The ability to interact well between compound molecules and target proteins was observed based on the free energy of bonds, hydrogen interaction of compound molecules, and inhibition concentration of compounds [43].

The molecular docking method has been validated using the enzyme alpha-glucosidase (PDB ID 2QMJ) and DPP-IV (PDB ID 5T4B) against each crystallographic ligand. The validation results show the proximity of the molecular docking results in the binding pocket of the target protein with the copy ligand and the crystallographic ligand with an RMSD value of < 2 Å. The results of the validation of the docking method on the target protein and ligand can be observed in Figure 4.

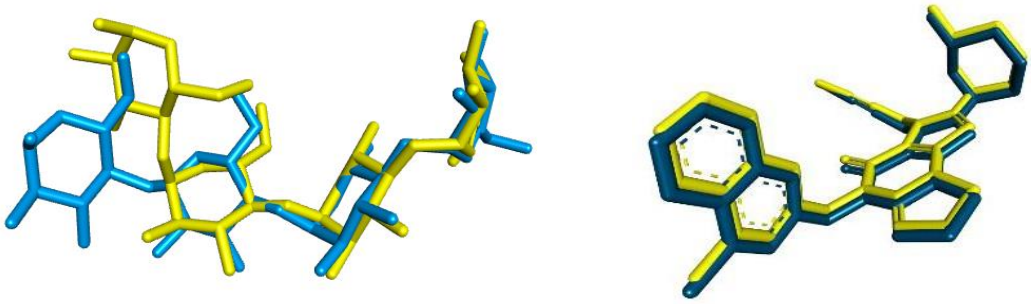

(a)

Figure 4. Visualization results of docking method validation on **(a)** alpha-glucosidase; **(b)** DPP-IV proteins. The RMSD value obtained between the copy ligand and the crystallographic ligand on the alpha-glucosidase protein is 1.28 Å, while on the DPP-IV protein, it is 0.37 Å. The crystallographic ligand (yellow) and ligand copy (blue).

The interaction between 29 compounds with the DPP4 enzyme showed that all compounds could interact with the active site of the DPP4 enzyme, which was marked by a negative Free Energy of Binding (FEB) (Table 5 and Table 6). The best interaction was shown by the compound 2-[4-(Diphenylmethyl)-1- piperazinyl] ethyl methyl 2,6-dimethyl-4-(3-nitrophenyl)-3,5-pyridinedicarboxylate and the compound (3β,16α,21β,22α)-16,21,22,24,28-Pentamethoxyolean-12-en-3-yl acetate from acetone extract with binding affinities of -11.77 and 10.64 kcal/mol, respectively. Meanwhile, the compounds from the ethyl acetate extract are the compounds (1R,3R,4S,5R)-3-[(E)-3-(3,4-dihydroxy phenyl)prop-2-enoyl]oxy-1,4-

hihydroxy-5-[E)-3-(4-hydroxy-3,5-dimethoxyphenyl)prop-2-enoyl]oxycyclohexane-1-carboxylate and the Linarin compound with binding affinities of -13.30 and -8.64 kcal/mol (Figure 5).

Table 5. The binding free energy of identified compounds from the acetone extract of Kesambi leaves against the target protein DPP-4.

No	Compounds	Free binding energy (Kcal/mol)	Amino acid residue
	2-[(3R)-3-aminopiperidin-1- yl]-3-(but-2-yn-lyl)-5- [(4methylquinazolin-2- yl)methyl]-3H-imidazo[2,1 b]purin-4(5H)-one (**Crystalography Ligan**)	-12.07	SER630, TYR547, GLU206, GLU205, TYR662, PHE357, VAL656, TYR666,HIS740, TYR631 VAL711, TRP629
1	Colcheine	-6.68	LYS554, TYR547, ASN710, TYR662, ARG125, HIS740, SER630, TRP629
2	D-(+)-Catechin	-6.27	TYR547, TRP629, GLY632, VAL546, TYR631, SER630, ARG125, ASN710, GLU205, TYR662, GLU206
3	Rhoifolin	-8.14	VAL546, GLY632, TRP629, GLY628, LYS554, TYR547, TYR631, SER630, TYR666, TYR662, VAL711, VAL656, ARG125, GLU205, GLU206
4	Podophyllotoxin glucoside	-6.45	SER630, TYR631, LYS554, VAL546, TRP629, TYR547, TYR666, ARG669, GLU206, PHE357, SER209, GLU205, HIS126, GLU204, ARG125
5	Metyl (1R,3R,4S,5R)-3-[(E)-3-(3,4-dihydroxyphenyl)prop- 2-enoyl]oxy-1,4-hihydroxy-5-[E)-3-(4-hydroxy-3,5- dimethoxyphenyl)prop-2-enoyl]oxycyclohexane-1-carboxylate	-13.30	SER630, TRP629, GLY632, VAL546, ASP545, GLY628, TRP627, TYR752, LYS554, TYR631, TYR547
6	5,7-Diacetoxy-3,4',8- trimethoxyflavone	-8.22	TYR547, SER630, TYR631, GLY632, TRP629, GLY628, ASP545, VAL546, LYS554, TRP627
7	Podophyllotoxin β-D- glucoside	-6.68	TRP629, GLY632, SER630, HIS740, ASN710, ARG125, GLU205, TYR662, GLU206, TYR666, PHE357, TYR547, SER552, GLN553, ASP556, ARG560, LYS554, VAL546
8	undeca-2,4,6-trienoic acid	-4.99	LYS554, VAL546, GLY628, TRP629, GLY632, TYR666, VAL656, TYR662, TYR547, SER630, TYR631
9	(-)-Podophyllotoxin	-6.47	SER630, TYR631, TYR547, GLY632, GLY628, VAL546, LYS554, TRP629
10	Dicoumarol	-7.83	SER209, GLU205, ASN710, ARG125, HIS740, SER630, VAL711, TYR666, VAL656, TYR662, TYR631, TYR547, GLU206, ARG669, PHE357
11	MFCD00152656	-4.59	TYR662, TYR631, TRP659, VAL656, TYR666, SER630, TYR547, GLY632, VAL546, TRP629, ASP545, LYS554, TRP627, GLY628
12	N-[(2S)-4-Amino-1-{[(2S)-1-amino-5-carbamimidamido-1- oxo-2-pentanyl]amino}-1-oxo- 2-butanyl]-N^2-(phenylacetyl)- L-lysinamide	-6.98	TRP627, VAL546, GLY628, ASP545, LYS554, TYR547, TYR666, PHE357, GLU206, GLU 205, TYR662, ASN710, TYR631, ARG125, SER630, HIS740, TRP629, GLY741
13	(3β,16α,21β,22α)-16,21,22,24,28-Pentamethoxyolean-12-en-3- yl acetate	-10.64	GLU205, ARG669, GLU206, TYR662, PHE357, TYR666, TYR631, SER630, TYR547, TRP629, VAL546, LYS554
14	2-[4-(Diphenylmethyl)-1- piperazinyl]ethyl methyl	-11.77	TYR547, GLY632, TYR631, TRP629,

No	Compounds	Free binding energy (Kcal/mol)	Amino acid residue
	2,6- dimethyl-4-(3-nitrophenyl)- 3,5-pyridinedicarboxylate		VAL546, TRP627, ASP545, SER630, ARG125, GLU205, GLU206, TYR662
15	Pheophorbide	-5.35	TRP629, GLY632, TYR547, TYR632,TYR662, VAL656, TYR666, SER630, GLU205, GLU206,ARG125
16	Bis[2-(4-butoxyphenoxy)ethyl] (4-hydroxybenzylidene)malonate	-10.11	GLY741, HIS740, ARG125, GLU205, GLU206, TYR666, TYR631, GLY632, TRP627, VAL546, ASP545, LYS554, TYR547, TRP629, SER630, TYR662, TYR752
17	L-Phenylalanine, N-[[(3S)-2-[(2S)-2-amino-3-(4-hydroxyphenyl)-1- oxopropyl]-1,2,3,4- tetrahydro-3-isoquinolinyl]methyl]-L- phenylalanyl	-0.83	TRP627, VAL546, GLY628, ASP545, LYS554, TRP629
18	Dulxanthone G	-7.52	TYR631, GLY632, VAL546, TRP627, TYR752, TRP629, TYR547, HIS740, ARG125, SER630, ASN710, TYR662, GLU205, GLU206
19	6-[(1,3-Dihydroxy-2- propanyl)amino]-12-(D-glucopyranosyl)-2-hydroxy-	-5.73	ARG125, LYS554, VAL546, GLY628, TRP629, GLY632,
20	L-Histidine trimethylbetaine	-4.15	GLU205, TYR662, GLU206, TYR666, TYR547, ARG125, HIS740, SER630, VAL711, VAL656, TYR631, TRP659
21	Nimbolinin D	-8.21	GLU205, ARG125, SER630, HIS740, TRP629, TYR631, TYR547, ASP545, VAL546, GLY628, TRP627, LYS554

Table 6. The binding free energy of identified compounds from the acetone extract of Kesambi leaves against the target protein DPP-4.

No	Compounds	Energy of binding (Kcal/mol)	Amino acid residue
	2-[(3R)-3-aminopiperidin-1-yl]-3- (but-2-yn-lyl)-5-[(4methylquinazolin-2- yl)methyl]-3H- imidazo[2,1 b]purin-4(5H)-one (**Crystalography ligand**)	-12.07	SER630, TYR547, GLU206, GLU205, TYR662, PHE357, VAL656, TYR666, HIS740, TYR631 VAL711, TRP629
22	Quercitrin	-6.80	TYR662, SER630, GLU205, ASN710, ARG125, HIS740, TYR547, LYS554, ASP545, VAL546, GLY628, TRP629, GLY632, TYR631, TYR666
23	Loliolide	-5.82	SER630, ARG125, HIS740, TYR631, PRO550, TYR547, GLY549,TYR666, TYR662
24	Linarin	-8.74	GLY741, TRP629, GLY632, TYR631, TRP659, SER630, VAL711,TYR666, VAL656, TYR547, GLU206, GLU205, TYR662, ARG125, TYR752
25	Metyl (1R,3R,4S,5R)-3-[(E)-3-(3,4-dihydroxyphenyl)prop-2-enoyl]oxy-1,4-hihydroxy- 5-[E)-3-(4-hydroxy-3,5-dimethoxyphenyl)prop-2- enoyl]oxycyclohexane-1-carboxylate	-13.30	SER630, TRP629, GLY632, VAL546, ASP545, GLY628, TRP627, TYR752, LYS554, TYR631, TYR547
26	Dulxanthone G	-7.52	TYR631, GLY632, VAL546, TRP627, TYR752, TRP629, TYR547, HIS740, ARG125, SER630, ASN710, TYR662, GLU205, GLU206
27	Annohexocin	-3.40	TRP627, LYS554, SER630, TYR631, GLU205, GLU206, ARG669, PHE357, TYR666, TYR662, TYR547, TRP629, VAL546, ASP545, GLY628
28	Muricoreacin	-7.27	ASN710, TYR662, ARG125, GLU205, GLU206, PHE357, ARG669, TYR666, TYR547, TYR631, TRP629, SER630, VAL546, LYS554, GLY632

No	Compounds	Energy of binding (Kcal/mol)	Amino acid residue
29	Corossolone	-6.10	TRP659, TYR666, TYR547, SER630, GLY632, VAL546, GLY628, ASP545, TYR752, HIS740, TRP629, LYS554, TRP627, ARG125, GLU206, PHE357, GLU205, TYR662, TYR631

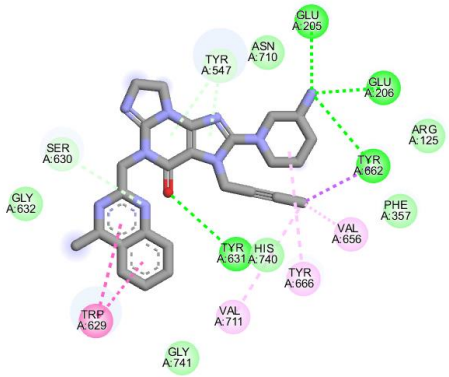

Ligand crystallography (binding affinity of -12.07)

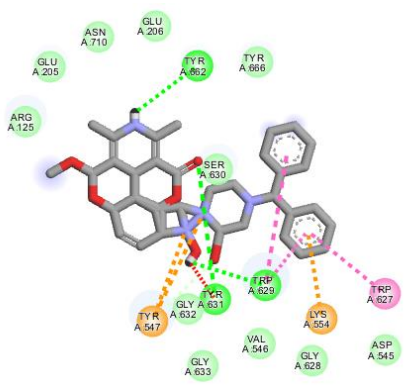

(14)

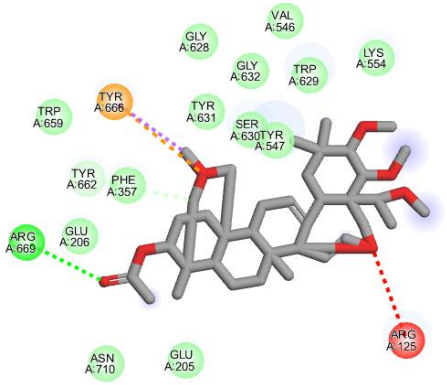

(13)

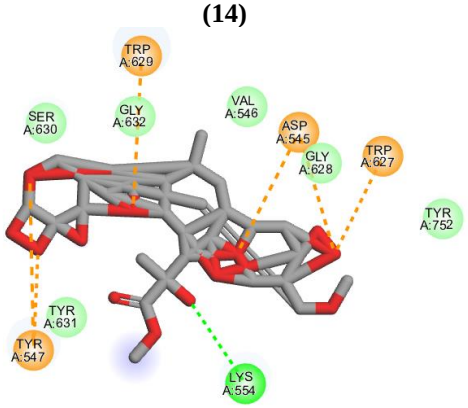

(25)

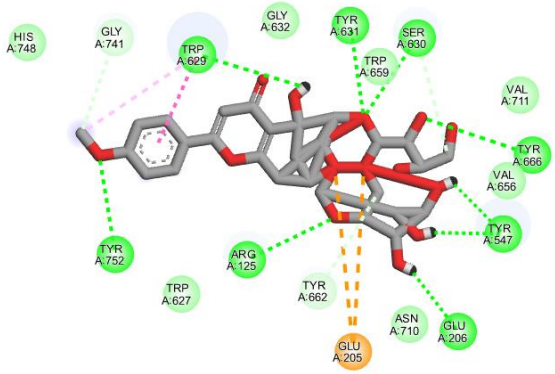

(24)

Figure 5. Visualization of the interaction between the target protein 5T4B (DPP-IV) and the active compounds **(14)** 2-[4-(diphenylmethyl)-1- piperazinyl] ethyl methyl 2,6-dimethyl-4-(3-nitrophenyl)-3,5-pyridine dicarboxylate and **(13)** (3β,16α,21β,22α)-16,21,22,24,28-Pentamethoxyolean-12-en-3-yl acetate from the acetone extract of Kesambi and **(25)** (1R,3R,4S,5R)-3-[(E)-3-(3,4-hydroxyphenyl)prop-2-enoyl]oxy-1,4-hyhydroxy- 5-[E)-3-(4-hydroxy-3,5-methoxyphenyl)prop-2-enoyl]oxycyclohexane-1-carboxylate and **(24)** Linarin from ethyl acetate extract of Kesambi.

The visualization results in Figure 5 show the negative affinity binding energy of the selected compounds that approach the affinity binding energy of the crystallographic ligand. In the interaction, it was found that the crystallographic ligand interacts with hydrogen on the amino acid residues GluA 205, GluA 206, TyrA 662, and TyrA 631. The closeness of the

interaction between the crystallographic ligand and the selected compounds (compounds 13, 14, 24, and 25). Selected compounds 13, 14, and 24 generally interact almost the same on the crystallographic ligand, namely on the amino acid residues TyrA 662 and TyrA 631. However, the interaction on compound C looks different and interacts with hydrogen on other amino acid residues. However, compound C has a more negative binding affinity than the crystallographic ligand. This activity suggests that the inhibition mechanism of these compounds is quite different. Compounds 13, 14, and 24 allow competitive inhibition of 5T4B protein because the interaction mechanism occurs at the same amino acid residue as the crystallographic ligand. In contrast, compound 25 allows non-competitive or even uncompetitive inhibition mechanisms. However, the prediction of the inhibition mechanism still needs to be studied further.

In the interaction of selected compounds with the target protein alpha-glucosidase (2QMJ) (Table 7 and Table 8), the three most active compounds were produced *in silico*. These compounds include **(5** and **25)** Methyl (1R,3R,4S,5R)-3-[(E)-3-(3,4-dihydroxyphenyl)prop-2-enoyl]oxy-1,4-hihydroxy-5-[E)-3-(4-hydroxy-3,5-dimethoxyphenyl)prop-2-enoyl]oxycyclohexane-1-carboxylate, which was found in acetone and ethyl acetate extracts of Kesambi leaves. Compound **(12)** N-[(2S)-4-Amino-1-{[(2S)-1-amino-5-carbamimidamido-1-oxo-2-pentanyl]amino}-1-oxo-2-butanyl]-N2-(phenylacetyl)-L-lysinamide found in the acetone extract of kesambi leaves and compound **(26)** Dulxanthone G found in the ethyl acetate extract of kesambi leaves with binding affinities of -11.03 (1), -8.46 (2), and -6.21 (3) respectively. Visualization of the interactions of the three compounds can be observed in Figure 6.

Table 7. The binding free energy of identified compounds from the acetone extract of Kesambi leaves against the target protein alfa-glucosidase.

No	Compounds	Energy of binding (Kcal/mol)	Amino acid residue
	Acarbose (Crystalography ligand)	-8-56	MET444, ASP203, ASP 443, ASP327, ASP542, TRP406, TRP539, TRP441, ARG526, HIS600, TYR299, PHE576, THR544, THR205, ALA576
1	Colchiceine	-6.97	ASP542, TYR299, TRP406, PHE450, ARG202, THR204, THR205, ALA576, SER448, ASP203, LYS480, PHE576
2	D-(+)-Catechin	-6.06	GLN603, GLY602, ASP203, ARG526, MET444, ILE364, ASP327, PHE575, TYR605, ASP542, ASP443, TRP406, TYR299
3	Rhoifolin	-5.88	ALA576, GLN603, PHE575, ASP542, TYR299, MET444, THR204, ARG202, LYS480, TYR605, ASP443, THR205, ASP203, TRP406
4	Podophyllotoxin glucoside	-7.93	THR205, PHE450, ASP203, ARG526, MET444, HIS600, PHE575, TRP406, GLY602, GLN603, ASP542, ASP443, ASP327, TYR299.
5	Methyl (1R,3R,4S,5R)-3-[(E)-3-(3,4-dihydroxyphenyl)prop-2-enoyl]oxy-1,4-hihydroxy-5-[E)-3-(4-hydroxy-3,5-dimethoxyphenyl)prop-2-enoyl]oxycyclohexane-1-carboxylate	-11.03	GLY602, PHE575, TRP406, PHE450, MET444, ARG526, ASP542, ASP203, TYR299, GLN603
6	5,7-Diacetoxy-3,4',8-trimethoxyflavone	-6.88	THR205, TYR299, PHE575, GLY602, ARG526, THR204, ARG202, LYS480, TRP406, MET444, ASP203, ASP542, ASP443, GLN603
7	Podophyllotoxin β-D-glucoside	-5.84	ASP443, THR204, GLY602, GLN603, TYR299, PHE450, LYS480, SER448, ARG202, ARG526, THR205, ASP203, MET444, ASP542, TYR605, PHE575, TRP406
8	undeca-2,4,6-trienoic acid	-4.43	THR204, ARG202, TRP406, ARG526, ASP54, ASP443, PHE575, MET444, THR205, ASP203
9	(-)-Podophyllotoxin	-6.07	THR204, ASP203, ASP542, ASP443, THR205, ARG202, LYS480, PHE450, ARG526, MET444, TRP406

No	Compounds	Energy of binding (Kcal/mol)	Amino acid residue
10	Dicoumarol	-6.86	MET444, ASP443, ILE364, TRP406, HIS600, TYR605, ILE328, ALA576, ASP327, TYR299, PHE575, ARG526, ASP542
11	MFCD00152656	-3.16	TRP406, ASP443, ASP327, ALA576, THR205, ASP542, ARG526, MET444, ASP366, ILE364, TRP441, ILE328, TYR299, HIS600, PHE575, ASP203, ASN543
12	N-[(2S)-4-Amino-1-{[(2S)-1-amino-5-carbamimidamido-1-oxo-2-pentanyl]amino}-1-oxo-2-butanyl]-N^2-(phenylacetyl)-L-lysinamide	-8.46	ASP443, TRP406, TYR299, ARG526, ILE364, HIS600, ILE328, THR204, PRO206, GLY602, GLN603, MET444, HE450, PHE575, ASP542, ASP203, ASP327, TYR214, THR205, TYR605
13	(3β,16α,21β,22α)-16,21,22,24,28-Pentamethoxyolean-12-en-3-yl acetate	-5.18	ASP542, PHE575, GLN603, TYR299, TRP406, LYS480, THR204, LEU473, ASP203, THR205
14	2-[4-(Diphenylmethyl)-1-piperazinyl]ethyl methyl 2,6-dimethyl-4-(3-nitrophenyl)-3,5-pyridinedicarboxylate	-10.70	ASP203, ARG526, TRP406, ASP327, GLN603, ASP542, THR205, ALA576, TYR299, PHE575, TYR605
15	Pheophorbide	-4.43	LEU473, ASN207, THR204, LYS480, LEU577, TYR605, PHE450, THR205, ARG202, ALA576, TYR299, PHE575, ASP2033
16	Bis[2-(4-butoxyphenoxy)ethyl] (4-hydroxybenzylidene)malonate	-6.16	ASP327, TRP406, PHE450, LYS480, TYR299, ARG202, THR205, THR204, PHE575, ASP203, ASP542, ARG526, ASP443. MET444
17	**L-Phenylalanine, N-[[(3S)-2-[(2S)-2-amino-3-(4-hydroxyphenyl)-1-oxopropyl]-1,2,3,4-tetrahydro-3-isoquinolinyl]methyl]-L-phenylalanyl**	-1.05	PHE576
18	Dulxanthone G	-6.21	ASP443, HIS600, ASP327, PHE575, TYR299, ARG526, ASP203, PHE450, TRP406, MET444, ASP542
19	6-[(1,3-Dihydroxy-2-propanyl)amino]-12-(D-glucopyranosyl)-2-hydroxy-12,13-dihydro-5H-indolo[2,3-a]pyrrolo[3,4-c]carbazole-5,7(6H)-dione	-4.34	ARG202, THR204, ASN449, SER448, PHE450, TRP406, TYR299, GLN603, PHE575, THR544, ASN543,ASP203, ALA576, LYS480, THR205, ASP542
20	L-Histidine trimethylbetaine	-4.01	THR204, SER448, LYS480, ASP542, THR205, ARG202, ASP203
21	Nimbolinin D	-6.82	THR544, ASN207, TYR605, GLY602, PHE575, TRP406, ARG526, MET444, ASP542, ASP203, THR204, LEU473, THR205, GLN603

Table 8. The binding free energy of identified compounds from the ethyl acetate extract of Kesambi leaves against the target protein alfa-glucosidase.

No	Nama senyawa	Binding energi	Asam amino
22	Quercitrin	-4.01	GLY602, TYR605, TYR299, PHE575, TRP539, TRP441, HIS600, MET444, PHE450, GLN603, ASP542, ASP327, SER448, ASP203
23	Loliolide	-5.61	HIS600, TRP441, ILE364, ASP443, ASP542, TRP539, ARG526, TRP406, PHE575, ASP327, TYR299
24	Linarin	-5.93	ARG202, THR204, TYR299, PHE575, GLY602, ALA576, ASP443, TRP406, ARG526, TYR605, GLN603, THR205, ASP203, ASP542, MET444, LYS480
25	Methyl (1R,3R,4S,5R)-3-[(E)-3-(3,4-dihydroxyphenyl)prop-2-enoyl]oxy-1,4-hihydroxy-5-[E)-3-(4-hydroxy-3,5-dimethoxyphenyl)prop-2-enoyl]oxycyclohexane-1-carboxylate	-11.03	GLY602, PHE575, TRP406, PHE450, MET444, ARG526, ASP542, ASP203, TYR299, GLN603
26	Dulxanthone G	-6.21	ASP443, HIS600, ASP327, PHE575, TYR299, ARG526, ASP203, PHE450, TRP406, MET444, ASP542
27	Annohexocin	-1.76	PHE450, LYS480, SER448, TYR605, ALA576, MET444, ASP542, TRP406, HIS600, PHE575, ASP327, TRP441, ASP443, TYR299, ARG526, GLN603, ASP203

No	Nama senyawa	Binding energi	Asam amino
28	Muricoreacin	-3.26	TRP441, ASP327, TYR299, TRP406, ASP542, THR544, THR205, TYR605, MET444, ASP571, PHE575, ALA576, HIS600, TRP539, ARG526, ASP203, GLN603
29	Corossolone	-3.11	PHE450, TRP406, TYR299, GIY602, THR205, TYR 605, ASP542, ASP203, ASP327, ASP443, ALA576, GLN603, PHE575

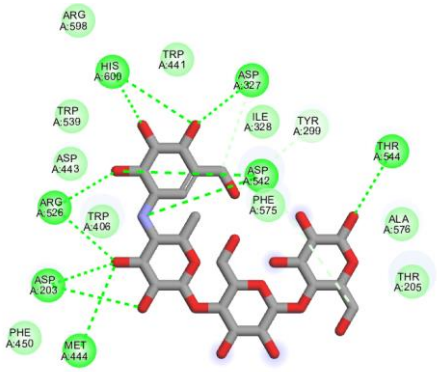

Crystalography ligand (-8.56)

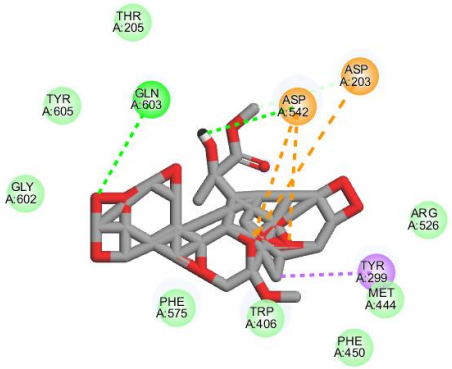

Compound 5 and 25

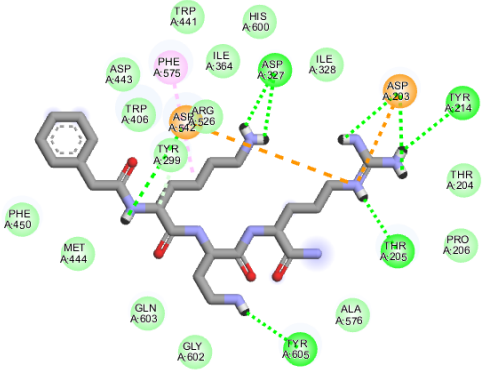

Compound 12

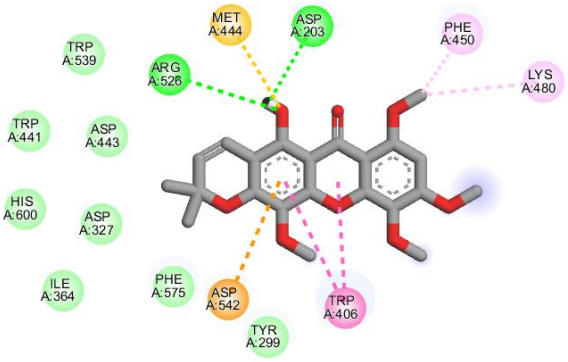

Compound 26

Figure 6. Visualization of the interaction between the target protein 2QMJ (alpha-glucosidase) and the active compounds **(5&25)** (1R,3R,4S,5R)-3-[(E)-3-(3,4-dihydroxyphenyl)prop-2-enoyl]oxy-1,4-hihydroxy-5-[E)-3-(4-hydroxy-3,5-dimethoxyphenyl)prop-2-enoyl]oxycyclohexane-1-carboxylate, **(12)** N-[(2S)-4-Amino-1-{[(2S)-1-amino-5-carbamimidamido-1-oxo-2-pentanyl]amino}-1-oxo-2-butanyl]-N^2-(phenylacetyl)-L-lysinamide, and **(26)** Dulxanthone G.

The docking visualization results from Figure 6 show the presence of a unique compound, namely compound **(5** and **25)** (1R,3R,4S,5R)-3-[(E)-3-(3,4-dihydroxy phenyl)prop-2-enoyl]oxy-1,4-hihydroxy-5-[E)-3-(4-hydroxy-3,5-dimethoxyphenyl)prop-2-enoyl]oxycyclohexane-1-carboxylate. The compound interacts strongly with the 2QMJ protein with a binding affinity of 11.03 kcal/mol. Compound (**5** and **25)** was identified as having a more negative binding affinity value compared to the crystallographic ligand of -8.56. The most negative binding affinity value indicates a strong interaction with the target protein. In crystallography ligands, identified hydrogen interactions are shown in amino acid residues Met 444, ArgA 526, AspA 203, AspA 327, AspA 542, ThrA 544, and HisA 600. However, in compounds 5 and 25, it was observed that overall, it binds to almost the identical amino acid residues of the crystallography ligand, although the type of interaction is slightly different. In Compounds 5 and 25, pi-cation (orange color) interacts with specific amino acid residues, AspA 542 and AspA 327, which, in crystallography, ligand hydrogen bonds to these amino acid residues. The difference in the type of bond allows its binding affinity to the target protein to be much more negative than the crystallography ligand [44,45]. Compounds 5 and 25 are also unique because they strongly interact with the target proteins alpha-glucosidase and DPP-

IV. Of course, this compound can be further developed and studied more deeply for its ability to inhibit multi-target proteins.

Other compounds, namely compounds **(12)** N-[(2S)-4-Amino-1-{[(2S)-1-amino-5-carbamimidamido-1-oxo-2-pentanyl]amino}-1-oxo-2-butanyl]-N2-(phenylacetyl)-L-lysinamide, and **(26)** Dulxanthone G, have also been observed to have the ability to inhibit the target protein alpha-glucosidase (2QMJ). Both compounds interact similarly with the identical amino acid residues as the crystallographic ligand. However, pi-cation interactions were also found at specific amino acid residues of the target protein, namely AspA 542, AspA 203, and Met 444. The three most active compounds are thought to be able to inhibit the alpha-glucosidase enzyme competitively based on observations of chemical interactions at the identical amino acid residues as the crystallographic ligand. However, the inhibitory mechanism of a chemical compound against the alpha-glucosidase enzyme still needs to be studied as a whole.

3.6. Molecular dynamics evaluation.

The results of molecular docking of compounds from the kesambi leaf extract that have been evaluated, it was decided that there were four active compounds *in silico* in inhibiting DPP-4, including the compound **(14)** 2-[4-(diphenylmethyl)-1- piperazinyl] ethyl methyl 2,6-dimethyl-4-(3-nitrophenyl)-3,5-pyridine dicarboxylate, compound **(13)** (3β,16α,21β,22α)-16,21,22,24,28-Pentamethoxyolean-12-en-3-yl acetate, **(5)** (1R,3R,4S,5R)-3-[(E)-3-(3,4-dihydroxy phenyl)prop-2-enoyl]oxy- 1,4-hihydroxy-5-[E)-3- (4-hydroxy-3,5-dimethoxyphenyl)prop -2-enoyl]oxycyclohexane-1-carboxylate, compound **(24)** linarin and three compound in inhibiting alpha-glucosidase, including **(5&25)** (1R,3R,4S,5R)-3-[(E)-3-(3,4-dihydroxyphenyl)prop-2-enoyl]oxy-1,4-hihydroxy-5-[E)-3-(4-hydroxy-3,5-dimethoxyphenyl)prop-2-enoyl]oxycyclohexane-1-carboxylate, **(12)** N-[(2S)-4-Amino-1-{[(2S)-1-amino-5-carbamimidamido-1-oxo-2-pentanyl]amino}-1-oxo-2-butanyl]-N^2-(phenylacetyl)-L-lysinamide, and **(26)** Dulxanthone G.

Through a molecular dynamics approach, the compounds were evaluated to stabilize their binding interactions against the target proteins alpha-glucosidase and DPP-IV. The stabilization of ligand binding to the target protein is evaluated using the Root Mean Square Deviation (RMSD), Root Mean Square Fluctuation (RMSF), and Radius of Gyration (RoS) parameters [43].

The results of the dynamic molecular analysis on the RMSD parameters were simulated for 100 ns. The simulation was carried out up to 100 ns because it could evaluate the conformational changes in the bonds [46,47]. The results of the RMSD simulation on the compound molecules and ligand crystallography can be observed in Figures 6a and 6b. The RMSD simulation on the four ligands (Figure 7a) experienced an increase in RMSD starting from 0 to 50 ns on the DPP-4 protein. The rise in backbone RMSD indicates that the enzyme structure begins to unfold [48]. The backbone RMSD of the four ligands began to stabilize at 60 ns until the end of the simulation (100 ns). This is because there has been interaction between residues in the enzyme, so the protein tends to maintain its structure at that stage [49]. Figure 7b is an RMSD simulation of the alpha-glucosidase protein.

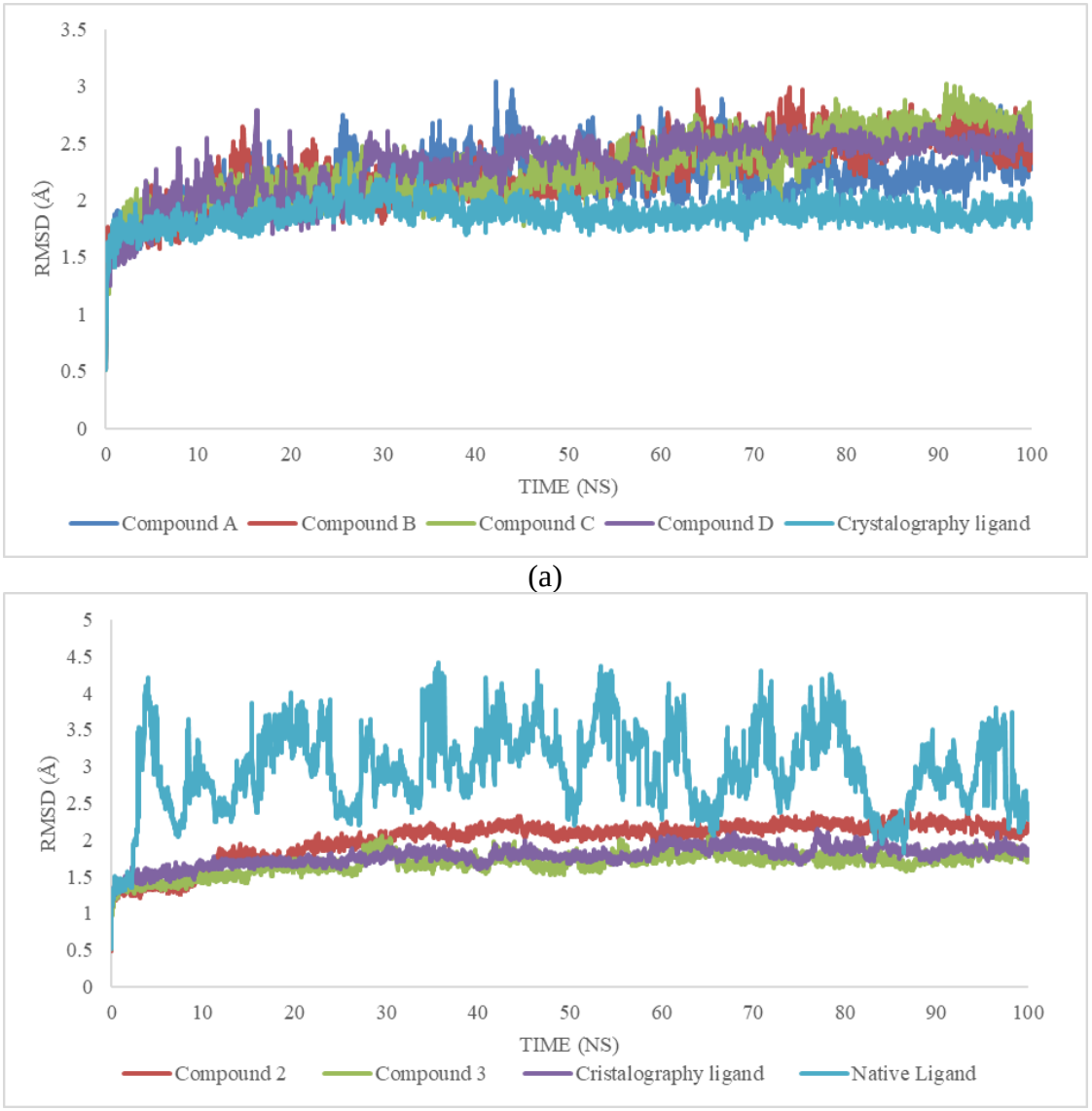

Figure 7. Visualization of RMSD of ligand compounds against **(a)** DPP-IV protein; **(b)** alpha-glucosidase.

The results of the RMSD simulation of the three ligands on the alpha-glucosidase protein show an increase in different RMSD values on the DPP-IV protein. The average increase in backbone RMSD in the four ligands generally occurs up to 30 ns and begins to stabilize at 40 ns until the end of the simulation. The RMSD values of the four ligands in DPP-IV and three ligands in alpha-glucosidase proteins until the end of the simulation were found to be values <2.5 Å to 2 Å. However, uniqueness occurs in the RMSD of the alpha-glucosidase protein, where the crystallographic ligand was found to have an RMSD value of >2.5 Å and was different from the three compound ligands. The compound's ligands showed better stability compared to the crystallographic ligands.

The potential energy of ligand binding to the target protein was also evaluated in this study using the RSMF approach. RMSF shows the fluctuation of amino acid residues that make up the receptor during the simulation process so that it can present the flexibility of the residues. The highest RMSF value in the system indicates an unstable amino acid bond that is difficult to bind, while a low RMSF value indicates that the compounds interact with a more stable bond [48,49].

RMSF was measured when the potential energy fluctuated from 1 ns until the simulation ended. Overall, there is low flexibility in the residue area that binds the ligand in

the area of 0.5 to 2 Å in both DPP-IV and alpha-glucosidase proteins Figure 8. Although in compounds A and D in the DPP-IV protein, there is a fluctuation in residue 239 with an RMSF value reaching >3 Å, until the end of ns, it returns to stability at RMSF < 2 Å. Similar fluctuations were also found in compounds 1 and 3 at residues around 300-400 of the alpha-glucosidase protein target, with an RMSF reaching 4 Å and returning to stability until the end of ns. Overall, the evaluated ligands showed good interaction stability.

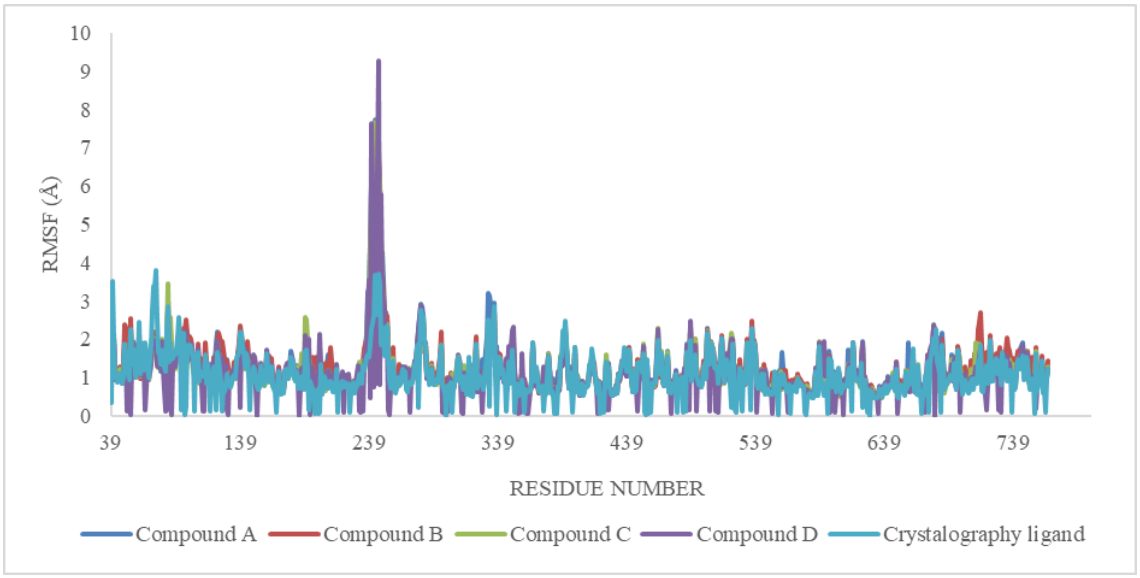

(a)

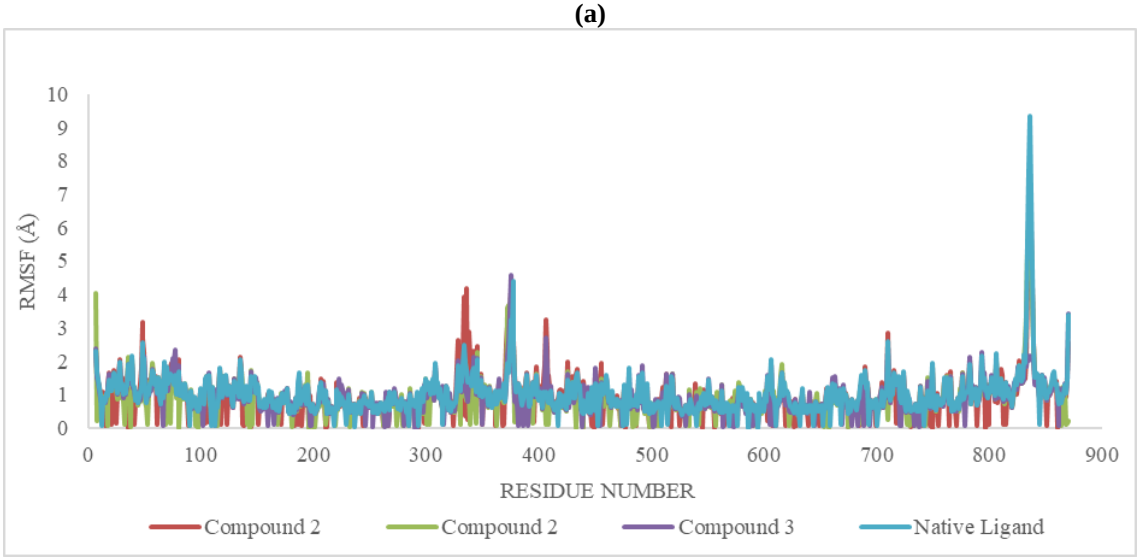

(b)

Figure 8. Visualization of RMSF of ligand compounds against **(a)** DPP-IV protein; **(b)** alpha-glucosidase.

The Radius of Gyration (RoG) parameter describes the complexation of protein structures [50]. The radii of gyration of both protein complexes in Figure 9 during the simulation are stable with each other. Although in the ligand complex of compound C with DPP-IV protein (Figure 9a), there is a fluctuation at 75 ns (orange graph), there is a change in the protein into an open-fold form. Still, it is stable again until the end of the simulation. Still, in the ligand-alpha glucosidase complex, it is observed to remain stable until the end of the simulation (Figure 9b). The stable RoG value is obtained below <28A in the ligand-protein complex of both enzymes. Based on the Radius of Gyration analysis, both are stable in terms of the compactness of the ligand-protein complex because only one fluctuation occurs, and the movement of the ligand-protein complex resembles each other.

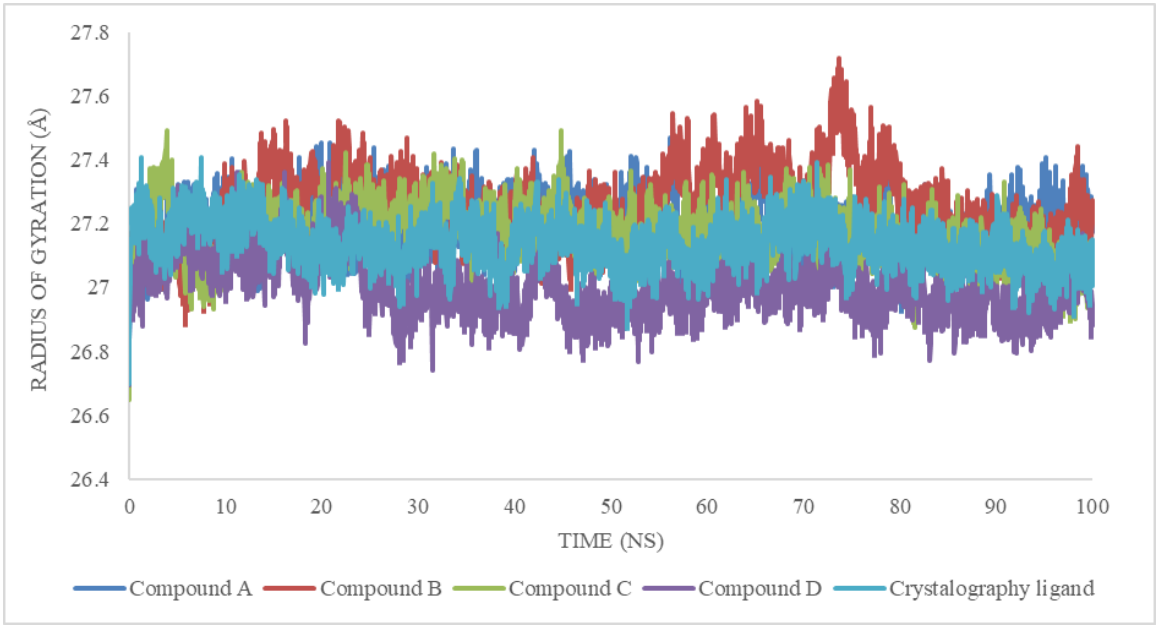

(a)

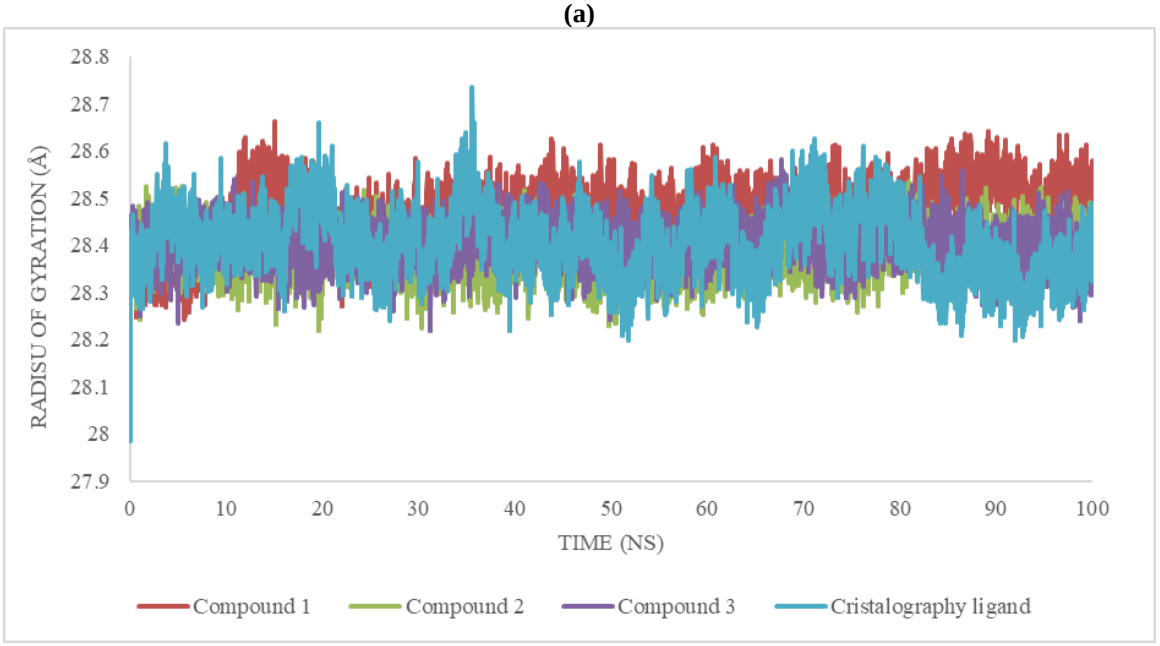

(b)

Figure 9. Visualization of the radius of gyration of ligand compounds against **(a)** DPP-IV protein; **(b)** alpha-glucosidase.

Overall, this study has provided an overview that Kesambi leaves can be used as a candidate raw material in diabetes therapy through the α-glucosidase and DPP-IV approaches. Although the antioxidant activity provided by each extract shows a strong ability, the mechanism has not fully provided a picture of its relationship to its activity as an antidiabetic. Hopefully, this study can be part of developing the Kesambi leaf extract in antidiabetic therapy. In the future, potential compounds from the active extract can be isolated and characterized to be used as markers for developing Kesambi leaf extract as a phytomedicine.

4. Conclusions

Ethyl acetate and acetone extracts of Kesambi leaves have been shown to have strong antioxidant capacity in reducing transition metals. In addition, acetone and ethyl acetate extracts also provide the ability as moderate to very strong alpha-glucosidase and DPP-4 inhibitors. The antioxidant and antidiabetic abilities of ethyl acetate and acetone extracts of

Kesambi leaves are influenced by secondary metabolites. Twenty-one compounds were identified in the acetone extract, and eight were identified in the ethyl acetate extract using the LC-ESI-MS approach. There are 7 compounds identified as having strong *in silico* interactions with the target proteins alpha-glucosidase (PDB ID 2QMJ) and DPP-IV (PDB ID 5T4B), including compound (14) 2-[4-(diphenylmethyl)-1- piperazinyl] ethyl methyl 2,6-dimethyl-4-(3-nitrophenyl)-3,5-pyridine dicarboxylate, compound (13) (3β,16α,21β,22α)-16,21,22,24,28-Pentamethoxyolean-12-en-3-yl acetate, (5) (1R,3R,4S,5R)-3-[(E)-3-(3,4-dihydroxy phenyl)prop-2-enoyl]oxy-1,4-hihydroxy-5-[E)-3-(4-hydroxy-3,5-dimethoxyphenyl)prop-2-enoyl]oxycyclohexane-1-carboxylate, compound (24) linarin and three compounds in inhibiting alpha-glucosidase, including (5&25) (1R,3R,4S,5R)-3-[(E)-3-(3,4-dihydroxyphenyl)prop-2-enoyl]oxy-1,4-hihydroxy-5-[E)-3-(4-hydroxy-3,5-dimethoxyphenyl)prop-2-enoyl]oxycyclohexane-1-carboxylate, (12) N-[(2S)-4-Amino-1-{[(2S)-1-amino-5-carbamimidamido-1-oxo-2-pentanyl]amino}-1-oxo-2-butanyl]-N2-(phenylacetyl)-L-lysinamide, and (26) Dulxanthone G. The stability of the bond between the identified compounds to the target protein through a molecular dynamic approach shows a stable and constant bond. Therefore, this study provides scientific information that the presence of compounds in the acetone and ethyl acetate extracts of Kesambi leaves can provide antioxidant and antidiabetic effects, so that they can be developed in future research.

Author Contributions

Conceptualization, NS. and S.N.; methodology, F.J.S. and H.K.; software, S.N.; validation, N.S., S.N., and H.K.; formal analysis, MW.; investigation, NS.; resources, MW.; data curation, F.J.S.; writing—original draft preparation, S.N.; writing—review and editing, N.S.; visualization, F.J.S.; supervision, NS.; project administration, H.K.; funding acquisition, NS. All authors have read and agreed to the published version of the manuscript.

Institutional Review Board Statement

Not applicable.

Informed Consent Statement

Not applicable.

Data Availability Statement

Data supporting the findings of this study are available upon reasonable request from the corresponding author.

Funding

This research was funded by Hibah Penelitian Fundamental (2024) from the Ministry of Education, Culture, Research, and Technology, Republic of Indonesia with contract No: 0459/E5/PG.02.00/2024 and Lembaga Penelitian dan Pengabdian Masyarakat Almarisah Madani University with contract No: 2893/UNIVERAL/LPPM/VI/2024.

Acknowledgments

The author would like to thank the Integrated Research Laboratory, Faculty of Health Sciences, Almarisah Madani University, Makassar, for the research facilities provided. The author would also like to thank the Kesambi Research Team, Ms. Yunita Sofyan, Ms. Dian Ekawati, and Mr. Abdul Azis, who helped complete this research.

Conflicts of Interest

The authors declare no conflict of interest.

References

1. Anjum, N.; Hossain, M.J.; Haque, M.R.; Chowdhury, A.; Rashid, M.A.; Kuddus, M.R. Phytochemical investigation of schleichera oleosa (lour.) oken leaf. *Bangladesh Pharm. J.* **2021**, *24*, 33-36, https://doi.org/10.3329/bpj.v24i1.51633.
2. Ghosh, P.; Chakraborty, P.; Mandal, A.; Rasul, M.G.; Chakraborty, M.; Saha, A. Triterpenoids from Schleichera oleosa of Darjeeling foothills and their antimicrobial activity. *Indian J. Pharm. Sci.* **2011**, *73*, 231, https://doi.org/10.4103/0250-474X.91568.
3. Silitonga, A.S.; Masjuki, H.H.; Mahlia, T.M.I.; Ong, H.C.; Kusumo, F.; Aditiya, H.B.; Ghazali, N.N.N. *Schleichera oleosa* L oil as feedstock for biodiesel production. *Fuel* **2015**, *156*, 63-70, https://doi.org/10.1016/j.fuel.2015.04.046.
4. Khandekar, U.; Bobade, A.; Ghongade, R. EVALUATION OF ANTIOXIDENT ACTIVITY, IN-VITRO ANTIMICROBIAL ACTIVITY AND PHYTOCONSTITUENTS OF *SCHLEICHERA OLEOSA* (LOUR.) OKEN. *Int. J. Biol. Pharm. Res.* **2015**, *6*, 137-143.
5. Nur, S.; Nursamsiar, N.; Khairuddin, K.; Megawati, M.; Fadri, A. PENENTUAN KADAR FLAVONOID DARI EKSTRAK ETANOL DAN ETIL ASETAT DAUN KESAMBI (Schleichera oleosa. L). *Acta Pharm. Indones.* **2021**, *46*, 33-37, https://doi.org/10.5614/api.v46i2.15772.
6. Rahayu, T.; Pratiwi, R.I.A.; Mubarakati, N.J. Metabolite Profiling of Schleichera oleosa Leaves Using Histochemical and *In silico* Analysis. *Metamorfosa: J. Biol. Sci.* **2021**, *8*, https://doi.org/10.24843/metamorfosa.2021.v08.i01.p17.
7. Nursamsiar, N.; Fadri, A.; Marwati, M.; Sami, F.J.; Ismail, N.S.H.R.; Kasmawati, H. Pengaruh Jenis Pelarut Terhadap Kadar Fenolik dan Flavonoid Total Daun Kesambi (Schleichera oleosa. L) Asal kabupaten Gowa. *Jurnal Mandala Pharmacon Indonesia* **2023**, *9*, 253-261, https://doi.org/10.35311/jmpi.v9i2.394.
8. Alim, N.; Hasan, T.; Rusman, R.; Jasmiadi, J.; Zulfitri, Z. Phytochemical Screening, Relationship of Total Phenolic with Antioxidant Activity Of Ethanol and Methanol Extracts of Kesambi (Schleichera oleosa (Lour.) Oken) Bark. *Jurnal Ilmiah Sains* **2022**, *22*, 118-124, https://doi.org/10.35799/jis.v22i2.40091.
9. Gulcin, İ. Antioxidants and antioxidant methods: an updated overview. *Arch. Toxicol.* **2020**, *94*, 651–715, https://doi.org/10.1007/s00204-020-02689-3.
10. Nur, S.; Hanafi, M.; Setiawan, H.; Elya, B. Chemical characterization and biological activity of *Molineria latifolia* root extract as dermal antiaging: Isolation of natural compounds, *in silico* and *in vitro* study. *Biocatal. Agric. Biotechnol.* **2024**, *56*, 103039, https://doi.org/10.1016/j.bcab.2024.103039.
11. Nur, S.; Setiawan, H.; Hanafi, M.; Elya, B. Phytochemical composition, antioxidant, *in vitro* and *in silico* studies of active compounds of *Curculigo latifolia* extracts as promising elastase inhibitor. *Saudi J. Biol. Sci.* **2023**, *30*, 103716, https://doi.org/10.1016/j.sjbs.2023.103716.
12. Nur, S.; Aisyah, A.N.; Lukitaningsih, E.; Juhardi, R.I.; Andirah, R.; Hajar, A.S. Evaluation of antioxidant and cytotoxic effect against cancer cells line of Angiopteris ferox Copel tuber and its compounds by LC-MS analysis. *J. Appl. Pharm. Sci.* **2021**, *11*, 054-061, https://doi.org/10.7324/JAPS.2021.110808.
13. Singh, A.-K.; Yadav, D.; Sharma, N.; Jin, J.-O. Dipeptidyl Peptidase (DPP)-IV Inhibitors with Antioxidant Potential Isolated from Natural Sources: A Novel Approach for the Management of Diabetes. *Pharmaceuticals* **2021**, *14*, 586, https://doi.org/10.3390/ph14060586.
14. Sekhon-Loodu, S.; Rupasinghe, H.P.V. Evaluation of Antioxidant, Antidiabetic and Antiobesity Potential of Selected Traditional Medicinal Plants. *Front. Nutr.* **2019**, *6*, 53, https://doi.org/10.3389/fnut.2019.00053.
15. Cecchini, S.; Fazio, F. Assessment of Total Antioxidant Capacity in Serum of Heathy and Stressed Hens. *Animals* **2020**, *10*, 2019, https://doi.org/10.3390/ani10112019.

16. Nur, S.; Aswad, M.; Yulianty, R.; Burhan, A.; Patabang, W.J.D.; Fadri, A.; Nursamsiar, N. Profil Aktivitas Antioksidan dari Ekstrak Buah Kersen (*Muntingia calabura* L.) dengan Metode TAC dan CUPRAC. *JPSCR: J. Pharm. Sci. Clin. Res.* **2022**, *1*, 79-88, https://doi.org/10.20961/jpscr.v7i1.56653.
17. Nur, S.; Setiawan, H.; Hanafi, M.; Elya, B. Pharmacognostical and Phytochemical Studies and Biological Activity of *Curculigo latifolia* Plant Organs for Natural Skin-Whitening Compound Candidate. *Sci. World J.* **2023**, *2023*, 5785259, https://doi.org/10.1155/2023/5785259.
18. Nur, S.; Wierson, Y.; Yulia, Y.; Sami, J.F.; Megawati, M.; Andi, N.A.; Marwati, M.; Gani, S.A. Characterization, Antioxidant and α-Glucosidase Inhibitory Activity of Collagen Hydrolysate from Lamuru (*Caranx ignobilis*) Fishbone. *Sains Malays* **2021**, *50*, 2329-2341, https://doi.org/10.17576/jsm-2021-5008-16.
19. Nursamsiar; Nur, S.; Febrina, E.; Asnawi, A.; Syafiie, S. Synthesis and Inhibitory Activity of Curculigoside A Derivatives as Potential Anti-Diabetic Agents with β-Cell Apoptosis. *J. Mol. Struct.* **2022**, *1265*, 133292, https://doi.org/10.1016/j.molstruc.2022.133292.
20. Muhammad Saiful, A.; Fadlina Chany, S.; Abdul, M.i. Inhibition of Dipeptidyl Peptidase 4 (DPP IV) Activity by Some Indonesia Edible Plants. *Pharmacogn. J.* **2019**, *11*, 231-236, http://dx.doi.org/10.5530/pj.2019.11.36.
21. Nur, S.; Hanafi, M.; Setiawan, H.; Nursamsiar, N.; Elya, B. Molecular Docking Simulation of Reported Phytochemical Compounds from Curculigo latifolia Extract on Target Proteins Related to Skin Antiaging. *Trop. J. Nat. Prod. Res.* **2023**, *7*, 5067–5080, http://www.doi.org/10.26538/tjnpr/v7i11.9.
22. Aristianti; Aswad, M.; Arsyad, A.; Nursamsiar; Nur, S.; Islam, A.A. THE POTENTIAL COMBINATION OF CENTELLA ASIATICA, CURCUMA LONGA, AND PIPER NIGRUM EXTRACTS IN TREATING BRAIN INJURY: *IN VITRO*, IN VIVO AND SILICO STUDIES. *Int. J. Appl. Pharm.* **2025**, *17*, 174-189, https://doi.org/10.22159/ijap.2025v17i2.53173.
23. Chemat, F.; Rombaut, N.; Sicaire, A.-G.; Meullemiestre, A.; Fabiano-Tixier, A.-S.; Abert-Vian, M. Ultrasound assisted extraction of food and natural products. Mechanisms, techniques, combinations, protocols and applications. A review. *Ultrason. Sonochemistry* **2017**, *34*, 540-560, https://doi.org/10.1016/j.ultsonch.2016.06.035.
24. Aisyah, A.N.; Lukitaningsih, E.; Rumiyati, R.; Marwati, M.; Sapra, A.; Khairi, N.; Fadri, A.; Nur, S. *In vitro* antioxidant and cytotoxic evaluation of ethyl acetate fraction of Angiopteris ferox Copel tuber against HTB lung cancer cell. *Egypt. J. Chem.* **2022**, *65*, 41-48, https://doi.org/10.21608/ejchem.2022.91843.4364.
25. Nur, S.; Hanafi, M.; Setiawan, H.; Elya, B. *In vitro* ultra violet (UV) protection of *curculigo latifolia* extract as a sunscreen candidate. *IOP Conf. Ser.: Earth Environ. Sci.* **2022**, *1116*, 012009, https://doi.org/10.1088/1755-1315/1116/1/012009.
26. Munteanu, I.G.; Apetrei, C. Analytical Methods Used in Determining Antioxidant Activity: A Review. *Int. J. Mol. Sci.* **2021**, *22*, 3380, https://doi.org/10.3390/ijms22073380.
27. Flieger, J.; Flieger, W.; Baj, J.; Maciejewski, R. Antioxidants: Classification, Natural Sources, Activity/Capacity Measurements, and Usefulness for the Synthesis of Nanoparticles. *Materials* **2021**, *14*, 4135, https://doi.org/10.3390/ma14154135.
28. Lfitat, A.; Zejli, H.; Bousraf, F.Z.; Bousselham, A.; El Atki, Y.; Gourch, A.; Lyoussi, B.; Abdellaoui, A. Comparative assessment of total phenolics content and *in vitro* antioxidant capacity variations of macerated leaf extracts of *Olea europaea* L. and *Argania spinosa* (L.) Skeels. *Mater. Today: Proc.* **2021**, *45*, 7271-7277, https://doi.org/10.1016/j.matpr.2020.12.990.
29. Sulistyowati; Elya, B.; Iswandana, R.; Nur, S. Phytocompounds and *in vitro* Antiaging Activity of Ethanolic Extract and Fractions of Rubus Fraxinifolius Poir. Leaves. [Fitocompuestos y actividad antienvejecimiento *in vitro* de extracto etanólico y fracciones de hojas de Rubus fraxinifolius Poir.]. *J. Pharm. Pharmacogn. Res.* **2023**, *11*, 595–610, https://doi.org/10.56499/jppres23.1614_11.4.595.
30. Holil, K.; Pramesti Griana, T. Analisis Fitokimia dan Aktivitas Antioksidan Ekstrak Daun Kesambi (Schleira oleosa) Metode DPPH. *J. Islam. Pharm.* **2020**, *5*, 28–32, https://doi.org/10.18860/jip.v5i1.9387.
31. Nursamsiar; Khairuddin; Marwati; Khairi, N.; Nur, d.S. ANTIOXIDANT ACTIVITIES OF ETHYL ACETATE EXTRACT OF KESAMBI (*Schleichera oleosa* L.) WITH DPPH METHOD. *Indones. J. Pharm. Sci. Technol.* **2024**, *11*, 1–8.
32. Maliki, I.; Moussaoui, A.E.; Ramdani, M.; Elbadaoui, K. Phytochemical screening and the antioxidant, antibacterial and antifungal activities of aqueous extracts from the leaves of Salvia officinalis planted in Morocco. *Moroc. J. Chem.* **2021**, *9*, 354–368, https://doi.org/10.48317/IMIST.PRSM/morjchem-v9i2.24840.

33. El Atki, Y.; Aouam, I.; El Kamari, F.; Taroq, A.; Zejli, H.; Taleb, M.; Lyoussi, B.; Abdellaoui, A. Antioxidant activities, total phenol an flavonoid contents of two Teucrium polium subspecies extracts. *Moroc. J. Chem.* **2020**, *8*, 446-455, https://doi.org/10.48317/IMIST.PRSM/morjchem-v8i2.17071.
34. Nur, S.; Angelina, A.A.; Aswad, M.; Yulianty, R.; Burhan, A.; Nursamsiar, N. *In vitro* anti-aging activity of *Muntingia calabura* L. fruit extract and its fractions. *J. Pharm. Pharmacogn. Res.* **2021**, *9*, 409-421.
35. Zabidi, N.A.; Akmal, I.N.; Muhajir, H.; Efliza, A.S.; and Mohammad Latif, M.A. Inhibitory evaluation of *Curculigo latifolia* on α-glucosidase, DPP (IV) and *in vitro* studies in antidiabetic with molecular docking relevance to type 2 diabetes mellitus. *J. Enzyme Inhib. Med. Chem.* **2021**, *36*, 109-121, https://doi.org/10.1080/14756366.2020.1844680.
36. Okechukwu, P.; Sharma, M.; Tan, W.H.; Chan, H.K.; Chirara, K.; Gaurav, A.; Al-Nema, M. *In-vitro* anti-diabetic activity and *in-silico* studies of binding energies of palmatine with alpha-amylase, alpha-glucosidase and DPP-IV enzymes. *Pharmacia* **2020**, *67*, 363-371, https://doi.org/10.3897/pharmacia.67.e58392.
37. Deacon, C.F. Physiology and Pharmacology of DPP-4 in Glucose Homeostasis and the Treatment of Type 2 Diabetes. *Front. Endocrinol.* **2019**, *10*, 80, https://doi.org/10.3389/fendo.2019.00080.
38. Mutha, R.E.; Tatiya, A.U.; Surana, S.J. Flavonoids as natural phenolic compounds and their role in therapeutics: an overview. *Futur. J. Pharm. Sci.* **2021**, *7*, 25, https://doi.org/10.1186/s43094-020-00161-8.
39. Shahidi, F.; Dissanayaka, C.S. Phenolic-protein interactions: insight from in-silico analyses – a review. *Food Prod. Process. Nutr.* **2023**, *5*, 2, https://doi.org/10.1186/s43014-022-00121-0.
40. Parcheta, M.; Świsłocka, R.; Orzechowska, S.; Akimowicz, M.; Choińska, R.; Lewandowski, W. Recent Developments in Effective Antioxidants: The Structure and Antioxidant Properties. *Materials* **2021**, *14*, 1984, https://doi.org/10.3390/ma14081984.
41. Yan, Z.; Zhong, Y.; Duan, Y.; Chen, Q.; Li, F. Antioxidant mechanism of tea polyphenols and its impact on health benefits. *Anim. Nutr.* **2020**, *6*, 115–123, https://doi.org/10.1016/j.aninu.2020.01.001.
42. L. Suraweera, T.; Rupasinghe, H.P.V.; Dellaire, G.; Xu, Z. Regulation of Nrf2/ARE Pathway by Dietary Flavonoids: A Friend or Foe for Cancer Management?. *Antioxidants* **2020**, *9*, 973, https://doi.org/10.3390/antiox9100973.
43. Nursamsiar; Siregar, M.; Awaluddin, A.; Nurnahari, N.; Nur, S.; Febrina, E.; Asnawi, A. MOLECULAR DOCKING AND MOLECULAR DYNAMIC SIMULATION OF THE AGLYCONE OF CURCULIGOSIDE A AND ITS DERIVATIVES AS ALPHA GLUCOSIDASE INHIBITORS. *Rasayan J. Chem.* **2020**, *13*, 690-698, https://doi.org/10.31788/RJC.2020.1315577.
44. Kumar, K.; Woo, S.M.; Siu, T.; Cortopassi, W.A.; Duarte, F.; Paton, R.S. Cation–π interactions in protein–ligand binding: theory and data-mining reveal different roles for lysine and arginine. *Chem. Sci.* **2018**, *9*, 2655-2665, https://doi.org/10.1039/c7sc04905f.
45. Dougherty, D.A. Cation-π Interactions Involving Aromatic Amino Acids [1 2 3 4]. *J. Nutr.* **2007**, *137*, 1504S-1508S, https://doi.org/10.1093/jn/137.6.1504S.
46. Schreiner, W.; Karch, R.; Knapp, B.; Ilieva, N. Relaxation Estimation of RMSD in Molecular Dynamics Immunosimulations. *Comput. Math. Methods Med.* **2012**, *2012*, 173521, https://doi.org/10.1155/2012/173521.
47. Ghahremanian, S.; Rashidi, M.M.; Raeisi, K.; Toghraie, D. Molecular dynamics simulation approach for discovering potential inhibitors against SARS-CoV-2: A structural review. *J. Mol. Liq.* **2022**, *354*, 118901, https://doi.org/10.1016/j.molliq.2022.118901.
48. Sang, P.; Du, X.; Yang, L.-Q.; Meng, Z.-H.; Liu, S.-Q. Molecular motions and free-energy landscape of serine proteinase K in relation to its cold-adaptation: a comparative molecular dynamics simulation study and the underlying mechanisms. *RSC Adv.* **2017**, *7*, 28580-28590, https://doi.org/10.1039/C6RA23230B.
49. Jairajpuri, D.S.; Mohammad, T.; Hussain, A.; Amir, S.; Fatima, U.; AlAjmi, M.F.; Yadav, D.K.; Hassan, M.I. An integrated docking and molecular dynamics simulation approach to discover potential inhibitors of activin receptor-like kinase 1. *J. Mol. Recognit.* **2024**, *37*, e3069, https://doi.org/ 10.1002/jmr.3069.
50. Lobanov, M.Y.; Bogatyreva, N.S.; Galzitskaya, O.V. Radius of gyration as an indicator of protein structure compactness. *Mol. Biol.* **2008**, *42*, 623-628, https://doi.org/10.1134/S0026893308040195.

Publisher's Note & Disclaimer